

Influence of initial soil moisture in a Regional Climate Model study over West Africa. Part 1: Impact on the climate mean

Brahima KONÉ¹, Arona DIEDHIOU^{1, 2}, Adama Diawara¹, Sandrine Anquetin², N'datchoh Evelyne Touré¹, Adama Bamba¹, and Arsene Toka Koba¹

¹LASMES - African Centre of Excellence on Climate Change, Biodiversity and Sustainable Agriculture (ACE CCBAD) / Université Félix Houphouët Boigny, Abidjan, Côte d'Ivoire

²Univ. Grenoble Alpes, IRD, CNRS, Grenoble INP, IGE, F-38000 Grenoble, France

Correspondence to: Arona DIEDHIOU (arona.diedhiou@ird.fr)

Abstract.

The impact of soil moisture initial conditions on the mean climate over West Africa was examined using the latest version of the Regional Climate Model of the International Centre for Theoretical Physics (RegCM4) at a horizontal resolution of 25 km × 25 km. The soil moisture reanalysis of the European Centre Meteorological Weather Forecast's reanalysis of the 20th century ERA20C is used to initialize the control experiment, while its minimum and maximum values over the entire domain are used to establish the initial dry and wet soil moisture conditions respectively (hereafter dry and wet experiments). For the control, the wet and dry experiments, an ensemble of five runs from June to September are performed. In each experiment, we analyzed the two idealized simulations most sensitive to the dry and wet soil moisture initial conditions. The impact of soil moisture initial conditions on precipitation in West Africa is linear over the Central and West Sahel where dry (wet) experiments lead to rainfall decrease (increase). The strongest precipitation increase is found over the West Sahel for wet experiments with a maximum change value of approximately 40%, while the strongest precipitation decrease is found for dry experiments over Central Sahel with a peak of change of approximately -4%. The sensitivity of soil moisture initial condition can persist for three to four months (90-120 days) depending on the region. However, the influence on precipitation is no longer than one month (between 15 and 30 days). The strongest temperature decrease is located over the Central and West Sahel with a maximum change of approximately -1.5 °C in wet experiments, while the strongest temperature increase is found over the Guinea Coast and Central Sahel for the dry experiments, with a maximum of change around 0.6°C. A significant

33 impact of soil moisture initial conditions on the surface energy fluxes is noted: in the wet (dry)
34 experiments, a cooling (warming) of surface temperature is associated with a decrease (increase)
35 of sensible heat flux, an increase (decrease) of latent heat flux and a decrease (increase) of the
36 boundary layer depth. Part II of this study investigates the influence of soil moisture initial
37 conditions on climate extremes.

38 **1 Introduction**

39 In the climate system, soil moisture is a crucial variable that influences water balance and
40 surface energy components through latent surface fluxes and evaporation. Therefore, soil
41 moisture impacts the development of weather patterns and precipitation. The strength of soil
42 moisture impacts on land-atmosphere coupling varies with location and season. Koster et al.
43 (2004) sustained that improving the simulation of the atmospheric response to the slow
44 variations of land and ocean surface conditions may be important for seasonal climate prediction.
45 The atmospheric response to ocean temperature anomalies has been well documented (Kirtman
46 et al. 1998; Rasmusson et al.1982). Schär et al. 1999 sustained that the role of soils may be
47 comparable to that of the oceans. The solar energy received by the oceans is stored in summer
48 and used to heat the atmosphere in winter. Conversely, the precipitation received by the soil is
49 stored in winter and the moistening (cooling) is returned to the atmosphere in summer. Through
50 its impact on surface energy fluxes and evaporation, there are many additional impacts on the
51 climate process of soil moisture, such as boundary-layer stability and air temperature (Hong and
52 Pan, 2000; Kim and Hong 2006). Several studies have shown that the anomalies of soil moisture
53 may persist for several weeks or months, however, its impact remains only for a shorter time in
54 the atmosphere, not exceeding few days (Vinnikov and Yesserkepova 1991; Liu et al., 2014). The
55 important role of anomalies in soil moisture in the coupling between land and atmosphere has
56 been shown in several studies, using numerical climate models (Zhang et al., 2011) and
57 observation datasets (Zhang et al., 2008a; Dirmeyer et al., 2006). For instance, over East Asia,
58 Zhang et al., (2011) showed that soil moisture is found to have a much stronger impact on daily
59 maximum temperature variability than on daily mean temperature variability, but generally has
60 small effects on daily minimum temperature, except in the eastern Tibetan Plateau. They showed
61 that soil moisture has a prominent contribution to precipitation variability in many parts of
62 western China.

63
64 West Africa is known to exhibit strong coupling between soil moisture and precipitation (Koster
65 et al., 2004). Several previous studies have been conducted over West Africa on a global scale

66 using atmospheric general circulation model (AGCMs) to investigate the impact of soil moisture
67 initial conditions on the land-atmosphere coupling (Koster et al., 2004; Douville and al, 2001;
68 Zhang et al., 2008b). However, at local and regional scales, the land-atmosphere coupling studies
69 with AGCMs, present significant uncertainties (Xue et al. 2010). The regional climate models
70 (RCMs) have been used to simulate the impact on interannual climate variability of anomalies in
71 soil moisture (Seneviratne et al. 2006; Zhang et al. 2011). These studies have received a lot of
72 attention due to the increase of climate variability associated with extreme weather events that
73 have greater societal and environmental impacts. In general, these studies have been conducted
74 in Asia, Europe and America (e.g. Seneviratne et al. 2006 for Europe; Zhang et al. 2011 for Asia;
75 Zhang et al. 2008b for America). Overall, the results of these studies showed that during
76 summer, the strong impact of the anomalies of soil moisture in land-atmosphere occurred mainly
77 over the transition zones with a climate between wet and dry regimes, in agreement with Koster
78 et al. (2004). The relevance and extent of this potential feedback are still poorly understood in
79 West Africa.

80 This study will focus on the influence of soil moisture initial conditions on climate mean. It is
81 based on performance assessment of the Regional Climate model version 4 coupled to the
82 version 4.5 of the Community Land Model (RegCM4-CLM4.5) performed by Koné et al. (2018)
83 where the ability of the model to reproduce the climate mean has been validated. The
84 descriptions of the model and experimental setup used in this study are presented in Section. 2;
85 in the Section 3, the influence of wet and dry soil moisture initial conditions on the subsequent
86 climate mean is analyzed and discussed; and in Section 4 the main conclusions are presented.
87 While this Part I investigates the impacts on the climate mean, the Part II of this article will be
88 focused on the influence of soil moisture initial conditions on climate extremes.

89 **2. Model and experimental design**

90 **2.1 Model description and observed datasets**

91 The fourth generation of the Regional Climate Model (RegCM4) of the International Centre for
92 Theoretical Physics (ICTP) is used in this study. Since its release, its physical representations
93 have been continuously developed and implemented. The version used in the present study is
94 RegCM4.7. The MM5 (Grell et al., 1994) non-hydrostatic dynamical core has been ported to
95 RegCM without removing the existing hydrostatic core. The model dynamical core used in this
96 study is non-hydrostatic. RegCM4 is a limited area model using a sigma pressure vertical grid
97 and the finite differencing algorithm of Arakawa B-grid (Giorgi et al., 2012). The radiation
98 scheme used in this version of RegCM4.7 is derived from the National Center for Atmospheric

99 Research (NCAR) Community Climate Model Version three (CCM3) (Kiehl et al., 1996).
100 Aerosols representation is from Zakey et al. (2006) and Solomon et al. (2006). The large-scale
101 precipitation scheme is from Pal et al. (2000) and the moisture scheme is the SUBgrid EXplicit
102 moisture scheme (SUBEX). The SUBEX take into account the sub-grid scale cloud variability,
103 and the accretion processes and evaporation for stable precipitation following the work of
104 Sundqvist et al., 1989. In the planetary boundary layer (PBL), the sensible heat over ocean and
105 land, water vapour and turbulent transport of momentum are calculated according to the
106 scheme of Holtslag et al. (1990). Heat and moisture, the momentum fluxes of ocean surfaces in
107 this study are computed as in Zeng et al. (1998). In RegCM4.7, convective precipitation and
108 land surface processes can be described by several parameterizations. Based on Koné et al.
109 (2018), we selected the convective scheme reported by Emanuel (1991) and the interaction
110 processes between soil, vegetation and atmosphere are parameterized with CLM4.5. In each
111 grid cell, CLM4.5 has 16 different Plant Functional Types (PFTs) and 10 soil layers (Lawrence
112 et al., 2011; Wang et al., 2016). RegCM4 is integrated over the domain of West Africa depicted
113 in Fig. 1 with 25 km (182x114 grid points; from 20° W-20° E and 5° S-21° N) with horizontal
114 resolution and with 18 vertical levels and the initial and boundary conditions are taken from the
115 European Centre for Medium-Range Weather Forecasts reanalysis (EIN75; Uppala et al., 2008;
116 Simmons et al., 2007). The sea surface temperatures are obtained from the National Oceanic
117 and Atmosphere Administration (NOAA) optimal interpolation weekly (OI_WK) (Reynolds et
118 al., 1996). The topography data are taken from the States Geological Survey (USGS) Global
119 Multi-resolution Terrain Elevation Data (GMTED; Danielson et al., 2011) at 30 arc-second
120 spatial resolution, which is an update to the Global Land Cover Characterization (GTOPO;
121 Loveland et al., 2000) dataset.

122 Our analysis focuses on precipitation and the 2 m air temperature over the West African domain
123 during the June-July-August-September (JJAS). We validate the simulated precipitation with the
124 dataset from the Climate Hazards Group Infrared Precipitation with Stations (CHIRPS)
125 developed at the University of California at Santa Barbara at the 0.05° high-resolution available
126 from 1981 to 2020 (Funk et al., 2015). The validation of the simulated 2 m temperature relies on
127 the CRU datasets (Climate Research Unit version 3.20) from the University of East Anglia,
128 gridded at a horizontal resolution of 0.5° for 1901 to 2011 (Harris et al., 2013). To facilitate
129 comparison between RegCM4 simulations, all products has been re-gridded to 0.22° × 0.22°
130 using a bilinear interpolation method (Nikulin et al., 2012).

131 **2.2 Experiments setup and analysis methodology**

132 The European 20th Century Weather Prediction Center ERA20C soil moisture reanalysis is used
133 to initialize the control experiment, while its domain-wide minimum and maximum values are
134 used to establish the initial dry and wet soil moisture conditions respectively (hereafter dry and
135 wet experiments). We initialized the dry and wet soil moisture initial conditions (in volumetric
136 fraction $\text{m}^3.\text{m}^{-3}$) respectively at the minimum value ($=0.117*10^{-4}$) and the maximum value
137 ($=0.489$).

138 We designed three experiments (reference, wet, and dry), each with an ensemble of five (5)
139 simulations starting from June 1st to September 30th. The difference between these three
140 experiments is the change in the initial soil moisture condition (reference initial soil moisture
141 condition, wet initial soil moisture condition, and dry initial soil moisture condition) during the
142 first day of the simulation (June 1st 2001, 2002, 2003, 2004 and 2005) over the West African
143 domain. Then, we selected the two runs most impacted by the wet and dry soil moisture initial
144 conditions in order to exhibit the effects on the climate mean beyond the limits of the impacts of
145 RegCM4 initial soil moisture internal forcing. In the same context, several previous studies have
146 selected two extreme years to investigate the climate models sensitivity to soil moisture initial
147 conditions (Hong et al., 2000; Kim and Hong, 2006) outside Africa.

148 Hong and al. (2000) used only two years (three months per year) to investigate the impact of
149 initial soil moisture over North America (in the Great Plains) during two summers spanning
150 May-June-July (MJJ) in 1988 (corresponding to a drought) and 1993 (corresponding to a
151 flooding event). Kim and Hong (2006) selected two contrasting years 1997 (below normal
152 precipitation) and 1998 (above normal precipitation year) for their study over east Asia. The first
153 seven days (Kang et al., 2014) are excluded from the analysis as a spin-up period. Except the
154 geographical location, the experimental setup is the same as that of Hong and Pan (2000). The
155 geographical location of this study is the same as in Koné et al. (2018), with four sub-regions
156 (Fig. 1) exhibiting different features of the annual precipitation cycle: Central Sahel ($10^\circ \text{W} - 10^\circ$
157 $\text{E}; 10^\circ \text{N} - 16^\circ \text{N}$), West Sahel ($18^\circ \text{W} - 10^\circ \text{W}, 10^\circ \text{N} - 16^\circ \text{N}$), and Guinea Coast ($15^\circ \text{W} - 10^\circ$
158 $\text{E}; 3^\circ \text{N} - 10^\circ \text{N}$).

159 In several previous studies (Liu et al., 2014; Hong and Pan, 2000; Kim and Hong, 2006), the
160 mean biases (MB) averaged over their studied domains are used to quantify the impact of the soil
161 moisture initial conditions. In our study, we used the MB and the probability density function
162 (PDF; Gao et al., 2016; Jaeger and Seneviratne, 2011) by fitting a normal distribution to better
163 capture how many grid points are impacted by soil moisture initial conditions. The pattern
164 correlation coefficient (PCC) is also used as a spatial correlation to reveal the degree of large-
165 scale similarity between model simulations and observations. These performance metrics (MB,

166 PCC, and PDF) are computed for both modeled and observed temperature and precipitation only
167 over land grid points.

168 For the two years most sensitive to soil moisture initial conditions, the Student t-test is used to
169 compare the significance of the difference between a wet or dry sensitivity test (sample 1) and
170 the control (sample 2) in assuming that our two samples are independent and in considering that
171 this method performs well for climate simulations compared to more sophisticated techniques
172 developed to address autocorrelation (Damien et al., 2014). The Student t-test is extensively used
173 for analysis in climate sciences; it is fairly robust and easy to use and interpret (Menedez et al.,
174 2019; Talahashi and Polcher, 2019). The Student t-test takes into account, the difference between
175 the means of each sample, the variance (S) and the number of degrees of freedom ($n - 1$), which
176 depends on the sample size (n). The test statistic is calculated as:

$$178 \quad t = \frac{\bar{X}_1 - \bar{X}_2}{\sqrt{\frac{S_1^2}{n_1} + \frac{S_2^2}{n_2}}}$$

177
179 Where \bar{X}_1 (\bar{X}_2) are the sample means, n_1 (n_2) are the sample sizes and S_1^2 (S_2^2) are the sample
180 variances. In this study, the t-test at the 95% confidence level is used to consider statistically
181 significant.

182

183 **3. Results and discussion**

184 **3.1. Influence of soil moisture initial conditions on precipitation.**

185 To identify the two runs most impacted by the dry and wet experiments among the ensemble of
186 five simulations (initiated on 1st June 2001, 2002, 2003, 2004 and 2005), we superimposed on
187 Figure 2, the magnitude of daily soil moisture changes of the 5 runs compared to their
188 corresponding control experiment over West African domain. Figure 2 shows that for the dry
189 experiments (negative values of daily soil moisture changes), the weakest and strongest impacts
190 of soil moisture initial conditions are found with the runs initiated on 1st June 2004 and 2003
191 respectively. For the wet experiments (positive values of daily soil moisture changes), the
192 weakest impact is found for the run initiated on 1st June 2003, while the other runs exhibit quite
193 the same strong sensitivity. From these results, we selected the two runs initiated on June 1st,
194 2003 and June 1st, 2004 as the simulations most influenced by the initial wet and dry soil
195 moisture conditions, respectively, to better highlight the effects on the climate mean beyond the
196 limits of the impact of the initial internal soil moisture forcing. It is worth noting that 2003 is

197 wetter than 2004 and is more sensitive to the dry experiment. While 2004 which is drier than
198 2003 is more sensitive to the wet experiment.

199
200 Figure 3 displays the spatial distribution of the observed mean rainfall (mm/day) from CHIRPS
201 (Fig. 3a, c) for the runs JJAS 2003 and JJAS 2004 and the simulated from control experiments
202 (Fig. 3b, d) initialized with reanalysis soil moisture ERA20C. Table 1 reports the MB and PCC
203 for model simulation compared to CHIRPS, computed for the Central Sahel, Guinea Coast, West
204 Sahel, and the entire West African domain. The CHIRPS product displays a zonal band of
205 rainfall centered around 10° N, decreasing from North to South (Fig. 3a, c). The maximum
206 values are located over the mountain regions of Cameroun and Guinea. While the precipitation
207 minimum values are found over the Sahel and the Sahara. The control experiments (Fig. 3 b and
208 d) reproduced the large-scale pattern of observed rainfall with PCC = 0.72 and 0.77 for the runs
209 JJAS 2003 and JJAS 2004, respectively (Table 1). The spatial extent of rainfall maxima and the
210 North-South gradient are well captured by control experiments; however, their magnitudes are
211 underestimated with respect to the CHIRPS observation. Over West African domain, dry MB
212 reaching -49.31% and -50.56% are obtained for the runs JJAS 2003 and JJAS 2004,
213 respectively (Table 1). Fig. 4 displays the change in mean precipitation (in %) in JJAS 2003 and
214 JJAS 2004 for dry and wet experiments with respect to the control experiments. The dotted area
215 shows changes with a statistical significance of 95%.

216
217 Dry and wet sensitivity experiments showed that precipitation is significantly affected by soil
218 moisture initial conditions at magnitude varying with the sub-regions (Fig. 4). Over the Central
219 Sahel, for the dry experiments (Fig. 4a, c), we found a precipitation decrease for JJAS 2003 and
220 JJAS 2004 (Fig. 4a, c). On the other hand, over the Guinea coast, we found an increase in rainfall
221 for both JJAS 2003 and JJAS 2004. For the wet experiments (Fig.4b, d), there is an increase of
222 rainfall over most of studied domains studied for both JJAS 2003 and JJAS 2004. Overall, the
223 impact of the soil moisture initial conditions on the precipitation is linear only over the Central
224 Sahel for both JJAS 2003 and 2004. Therefore, the dry (wet) experiments exhibits significant
225 decrease (increase) in precipitations with respect to the control experiments (Fig.4a, c).

226
227 For a better quantitative evaluation, the PDF distributions of precipitation changes in JJAS 2003
228 and JJAS 2004, over (a) central Sahel, (b) west Sahel, (c) Guinea coast and (d) West Africa
229 obtained from dry and wet experiments with respect to the control experiments are shown in Fig.
230 5. Table 2 summarizes the maximum values of changes obtained from the PDF's of the different

231 variables used in this study. The impact on precipitation of the soil moisture initial conditions is
232 linear only over Central Sahel (Fig.5a) where the change in dry (wet) experiments showed a
233 precipitation decrease (increase). The strongest precipitation increase is found over West Sahel
234 for the wet experience with maximum change reached 40%. However, the strongest precipitation
235 decrease is found over the Central Sahel for dry experiment with a maximum change value about
236 -4% (Table 2). We noted that the impacts on precipitation of the wet experiments are greater
237 than those from dry experiments (Table 2). These results are consistent with previous studies that
238 supported a strong relationship between precipitation and soil moisture in particular over the
239 transition zones with a climate between wet and dry climate regimes (Koster et al., 2004; Liu et
240 al., 2014; Douville et al., 2001).

241
242 Fig. 6 and Fig. 7 shows the changes in the daily soil moisture and precipitation, respectively,
243 from dry and wet experiments with respect to the control experiments, during the runs JJAS
244 2003 and JJAS 2004. To compute the changes of daily soil moisture, we considered the second
245 top soil layer in CLM4.5 (from 0 to 2.80 cm). In general, the impacts of soil moisture initial
246 conditions on the daily soil moisture persist from three to four months over the studied domains
247 (Fig.6). The strongest duration and amplitude of the impact on the daily soil moisture is found
248 over the West Sahel sub-region. The impact on the daily soil moisture lasts four months in JJAS
249 2003 and JJAS 2004. For wet experiments, the weakest duration of the impact of soil moisture
250 initial conditions is found over the Guinea Coast and lasts three months (Fig. 6c). While, for dry
251 experiments, the weakest impact on the daily soil moisture is found over Central Sahel and lasted
252 three months (Fig. 6a). These results are in line with previous works which argued that the soil
253 moisture-atmosphere feedback strength and the land memory are place dependent (Vinnikov et
254 al. 1996; Vinnikov and Yeserkepova 1991).

255 Figure 7 shows the changes of the daily precipitation to the soil moisture initial conditions over
256 the different studied domains. The impact of the wet experiments on daily precipitation is greater
257 in magnitude than that of dry experiments over most studied domains (Fig. 7). For dry
258 experiments, the strongest daily precipitation response (about $-4\text{mm}\cdot\text{day}^{-1}$), is found over the
259 Guinea Coast in the run JJAS 2003 (Fig. 7c). While for the wet experiments, the strongest impact
260 on the daily precipitation is more than $8\text{mm}\cdot\text{day}^{-1}$ and it is found over the West Sahel and the
261 Guinea Coast (Fig. 7b, c, respectively). It is worth to note that the impact of initial soil moisture
262 conditions on daily precipitation is much shorter than the duration of the impact on daily soil
263 moisture. The significant impact on daily precipitation is found only for wet experiments, and
264 did not last more than 15 days in large parts of the study domain, excepted over wetter sub-

265 region of Guinea Coast where it lasts approximately one month. We noted that the precipitation
266 peaks over West Sahel and Guinea Coast (Fig. 7b and c, respectively) during August and
267 September coincide with fluctuation in the daily soil moisture impact (Fig.6b and c). This
268 probably indicates the strong feedback of soil moisture and precipitation during this period over
269 the Guinea Coast and West Sahel regions.

270 To investigate the causes of the precipitation changes, we examined the vertical profile change in
271 relative humidity and air temperature for the runs JJAS 2003 and JJAS 2004, respectively, from
272 dry and wet experiments with respect their control experiment.

273 The impacts on relative humidity and air temperature (Fig.8 and Fig.9, respectively) of soil
274 moisture initial conditions are significant in the lower troposphere. In the low and mid-
275 troposphere, a drying and a warming are found in the dry experiments, while a moistening and a
276 cooling are simulated in the wet experiments. This indicates that a weak (strong) dry convection
277 is found over most of the studied domains for dry (wet) experiments. The strongest impact on the
278 relative humidity and temperature in the lower and middle troposphere is found over central
279 Sahel (Fig.8a and Fig. 9a).

280 For the upper troposphere, the significant impact on relative humidity and temperature is found
281 only for wet experiments, and exhibited a drying and a warming over most of studied domains
282 (Fig.8 and Fig.9). This impact for the wet experiments was also reported by Hong and Pal
283 (2000).

284 To understand other causes of the precipitation changes illustrated in Fig. 4, we analyzed the
285 changes in lower tropospheric wind (850hpa) and specific humidity for the runs JJAS 2003 and
286 JJAS 2004 during the dry and wet experiments with respect to the control experiments (Fig. 10).

287 For the dry experiments (Fig. 10a, c), we found that the moistening of the lower atmosphere
288 decreases over most of the study domain. However, the strong wind magnitude changes over the
289 Atlantic Ocean bring the moistening from the ocean to the Guinea Coast and West Sahel. This
290 can explain the precipitation increase over these sub-regions in the dry experiments. Over
291 Central Sahel, the strong decrease in precipitation seems to be associated with the decrease of
292 specific humidity which is particularly notable in the run JJAS 2003 (Fig.4a). Conversely, for the
293 wet experiments (Fig.10b, d), an increase in the moistening of the atmosphere is found mainly
294 over the Sahel band while further South, a decrease of the specific humidity is simulated over
295 Guinea Coast. The strong change in wind magnitude shifts the moistening from the North to the
296 South, leading to precipitation increase over most part of study domain (Fig.4 b and d). These
297 results are broadly consistent with precipitation changes for dry and wet experiments shown in
298 Figure 4.

299 Summarizing these results, the impact of soil moisture initial conditions is linear only over the
300 Central Sahel for the runs JJAS 2003 and 2004. The strongest precipitation decrease is found
301 over Central Sahel for the dry experiment in the run JJAS 2003 with maximum change reaching
302 -4% . While, the strongest precipitation increase is found over the West Sahel for the wet
303 experiment in the run JJAS 2004 with maximum change about 40% . The impact of soil moisture
304 initial conditions on daily soil moisture can persist for three to four months according to the sub-
305 domains, while the significant impact on precipitation (greater than $1\text{mm}\cdot\text{day}^{-1}$) is much shorter
306 and no longer than one month. The impact of soil moisture initial conditions is mostly confined
307 at the near-surface climate and somewhat at the upper troposphere.

308 **3.2. Influence on temperature and other surface fluxes.**

309 Figure 11 shows the spatial distribution of the mean observed 2m temperature from CRU during
310 JJAS 2003 and JJAS 2004 (Fig. 11a, c, respectively) and the mean simulated temperature from
311 the control experiments of runs JJAS 2003 and JJAS 2004 (Fig.11 b, d, respectively) initialized
312 with ERA20C. Table 3 summarizes the PCC and MB between model simulations of temperature
313 with respect to CRU, calculated for the West Sahel, Central Sahel, Guinea Coast and the entire
314 West African domain. The CRU temperature displays a zonal distribution over the whole West
315 Africa domain. Maximum values of approximately $34\text{ }^{\circ}\text{C}$ are found over the Sahara, while the
316 lowest temperatures not exceed 26°C , are located over the Guinea Coast especially in orographic
317 regions such as Guinean highlands, Cameroon Mountains and the Jos Plateau. The control
318 experiments (Fig. 11b, d) showed good agreement in the representation of the large-scale pattern
319 of CRU observation, with PCC about 0.99 for both JJAS 2003 and JJAS 2004 (Table 3),
320 including the meridional gradient between Sahara Desert and Guinea Coast which is crucial for
321 the African Easterly Jet evolution and formation (Thorncroft and Blackburn 1999; Cook 1999).
322 The spatial extent of temperature maxima and minima are well reproduced by control
323 experiments, however their magnitudes are overestimated compared to CRU. The strongest
324 warm MB of control experiments relative to CRU are approximately $2.68\text{ }^{\circ}\text{C}$ and $2.14\text{ }^{\circ}\text{C}$
325 respectively for JJAS 2003 and JJAS 2004; they are found over the West Sahel (Table 3).

326 Figure 12 shows changes in mean temperature for the runs JJAS 2003 and JJAS 2004 of dry and
327 wet experiments with respect to the control experiments. The dots show areas where impacts of
328 soil moisture initial condition are statistically significant at the 0.05 level. In the dry experiments,
329 for both JJAS 2003 and JJAS 2004 runs, the warmest changes are located under the latitude 13°
330 N, with maximum values located over the Guinea coast. For the wet experiments, the coolest
331 changes are found over the West and Central Sahel.

332 For a better quantitative evaluation, the PDF distributions of the changes in mean temperature in
333 runs JJAS 2003 and JJAS 2004 are showed in Figure 13. The impact on temperature is linear
334 over the Central Sahel, Guinea Coast and the whole West African domain (Fig.13a, c and d). The
335 strongest mean temperature decrease is observed over the Central and West Sahel in wet
336 experiences with the maximum change approximately -1.5 °C (Table 2). However, the strongest
337 increase of mean temperature is found over the Central Sahel (JJAS 2003) and the Guinea coast
338 (JJAS 2004) in dry experiments reaching 0.56 °C and 0.59 °C, respectively (Table 2). Overall,
339 the impact in the dry (wet) sensitivity experiments on 2m-temperature showed an increase
340 (decrease) in warming (cooling) for both JJAS 2003 and JJAS 2004 over most of the studied
341 domains. The exception is found over the west Sahel, where both dry and wet experiments lead
342 to temperature increase (Fig.13, Table2).

343 We now analyze the influence of soil moisture initial conditions anomalies on land energy
344 balance, particularly on the surface fluxes sensible and latent heat. Figure 14 shows changes in
345 sensible heat fluxes (in $W.m^{-2}$) in runs JJAS 2003 and JJAS 2004, from dry and wet experiments
346 compared to the control experiments. The dots show changes that are statistically significant at
347 the 0.05 level. As shown in figure 14, the impact on sensible fluxes of soil moisture initial
348 conditions is strong. It is linear over most of the studied domains: the dry (wet) experiments with
349 respect to the control exhibits significant increase (decrease) of the sensible heat (Fig.14).

350 The PDF distributions of change in sensible heat flux are displayed in Figure 15. The dry (wet)
351 experiments showed an increase (a decrease) of the sensible flux in both runs JJAS 2003 and
352 JJAS 2004 (Fig. 15). The impact in wet experiments is strong over Central and West Sahel
353 compared to the dry experiments, but not for Guinea Coast (Fig. 15, Table 2). In the dry
354 experiments, the strongest sensible heat flux increase is found over Guinea Coast, with
355 maximum change about 9.18 $W.m^{-2}$ during JJAS 2004 (see Table 2). In the wet experiments, the
356 strongest sensible heat flux decrease is located over Central Sahel with maximum change about
357 -39.66 $W.m^{-2}$ during JJAS 2003 (see Table 2).

358
359 Unlike the case of sensible heat flux, changes in latent heat showed a linear opposite patterns.
360 Dry experiments result in latent heat flux decrease, while the wet experiments result in latent
361 heat flux increase over most of studied domains (Fig. 16). The PDF distributions of latent heat
362 flux changes are shown in Figure 17. In the wet experiments, the strongest latent heat flux
363 increase is found over West Sahel with maximum change reaching 36.49 $W.m^{-2}$ in JJAS 2004
364 (Table2). In the dry experiments, the strongest latent heat flux decrease is located over Guinea
365 Coast with maximum change reaching -14.64 $W.m^{-2}$ in JJAS 2004 (Table2). It is worth to note

366 that the impacts on latent and sensible heat flux in wet experiments are stronger compared to
367 those in the dry experiments over most of studied domains, except over Guinea Coast (Table 2).

368
369 To determine whether most changes in energy go to evaporating water or to heating in the
370 surface boundary layer, we analyzed changes in Bowen ratio in runs JJAS 2003 and JJAS 2004,
371 for dry and wet experiments with respect to the control experiments (Fig. 18). The dots display
372 areas with statistically significant differences at the 0.05 level. The soil moisture initial
373 conditions strongly impact the Bowen ratio. Under the latitude 15°N, in the dry (wet)
374 experiment, the Bowen ratio values are in the range [0,1] ([-1;0]) meaning that the dry (wet)
375 experiments lead to an increase (decrease) of energy going to evaporate water. The exception is
376 found only over the West Sahel (Fig.18b). In the dry (wet) experiments, the areas with increase
377 (decrease) of energy going to evaporate water coincide with the areas of increase (decrease) of
378 temperature. However, over the Sahara and the West Sahel, most of energy is going to heating,
379 with Bowen ratio values out of the range [-1;1].

380 For a quantitative evaluation, the PDF distribution of the Bowen ratio is showed on Figure 19. In
381 the wet experiments, the decrease of Bowen ratio is associated with a decrease in the sensible
382 heat flux with the highest changes of energy conversion to heating simulated over West Sahel in
383 the run JJAS 2003. In the other subdomains, latent heat flux presents a higher increase than than
384 sensible heat flux which decreases compared to the control (Fig.19, Table 2). In the dry
385 experiments, there is an increase of sensible heat flux in the whole domain associated with an
386 increase of latent heat flux.

387
388 We then examined the impact on the stability of the PBL of the soil moisture initial conditions.
389 Different spatial distributions of surface fluxes significantly affect the boundary layer
390 development. Soil moisture can influence rainfall by limiting evapotranspiration, which affects
391 the development of the daytime PBL and thereby the initiation and intensity of convective
392 precipitation (Eltahir, 1998). Figure 20 shows changes in PBL (in m) for JJAS 2003 and JJAS
393 2004, from dry and wet experiments with respect to the control experiments with dotted areas
394 that are statistically significant at the 0.05 level. The soil moisture initial conditions impact
395 significantly the PBL. The dry experiments show PBL increase under the latitude 15 °N for both
396 JJAS 2003 and JJAS 2004 (Fig.20 a and c, respectively). For the wet experiments, a PBL
397 decrease is found over most of the studied domains. The PDF of PBL changes (Fig. 21) show
398 that the impact on PBL is linear over most of studied domains. The dry (wet) experiments lead to
399 an increase (decrease) of PBL for both JJAS 2003 and JJAS 2004. The strongest PBL increase

400 (decrease) is found over Guinea Coast (West Sahel) in dry (wet) experiments during JJAS 2004
401 (JJAS 2003) reaching 146.80m (-293.23m). A dry (wet) air is located above the areas where
402 PBL increase (decrease), causing the air column to become warm (cool) and dry (moist) for the
403 dry (wet) experiment (see Fig. 8 and Fig. 9). These results are consistent with the work of Hong
404 and Pan (2000).

405 Summarizing the results of this section, we found that in the wet experiments, the cooling of the
406 mean temperature is associated with an increase of the latent heat flux, a decrease of the sensible
407 heat flux and of the PBL depth over most studied domain. Conversely, in the dry experiments,
408 the warming of surface temperature is associated with a decrease of latent heat, an increase of
409 sensible heat flux and of PBL depth.

410 **4. Conclusion**

411 The impact of the soil moisture initial conditions on the subsequent summer (JJAS) mean
412 climate over West Africa was explored using the RegCM4-CLM45. In particular, the aim of this
413 study was to investigate how soil moisture initialization at the beginning of the rainy season may
414 affect the intra-seasonal variability of temperature and precipitation mean within the subsequent
415 season (June to September).

416 For this purpose, we set up three numerical experiments with RegCM4 in which we applied, at
417 the first day (June 1st), a control soil moisture initial condition (control experiment), a wet soil
418 moisture initial condition (wet experiment), and a dry soil moisture initial condition (dry
419 experiment). For each experiment, an ensemble of five simulations beginning from June 1st to
420 September 30th(JJAS), for the years 2001 to 2005 is performed. In this paper, we present results
421 of the two runs JJAS 2003 and JJAS 2004 most impacted by soil moisture dry and wet initial
422 conditions respectively to avoid effects of initial soil moisture internal forcing.

423 The impact of soil moisture initial conditions on precipitation is linear only over the Central
424 Sahel for both JJAS 2003 and JJAS 2004, and over the West Sahel especially in JJAS 2004. In
425 the dry experiment, the strongest precipitation decrease is found over the Central Sahel in JJAS
426 2003 with maximum change reaching -4% while in the wet experiment, the strongest
427 precipitation increase is found over the West Sahel in JJAS 2004 with maximum change
428 reaching 40%. The impact of soil moisture initial conditions can persist for three to four months
429 (90-120 days) depending on the sub-region but the impact on precipitation is no longer than 30
430 days (15 days over the Sahel and 30 days over the Guinea Sahel).

431 Our results show that soil moisture wet initial conditions lead in the lower troposphere to an
432 increase of relative humidity associated with a cooling of air temperature and in the upper
433 troposphere, to a decrease of relative humidity and a warming of air temperature. While the dry
434 experiments mainly impact the lower troposphere with a decrease of the relative humidity
435 associated with a warming air temperature.

436 The temperature at 2m is more sensitive to the anomalies of initial soil moisture condition than
437 the precipitation. The strongest impact on 2m-temperature is found over the Central Sahel with a
438 maximum change about $-1.5\text{ }^{\circ}\text{C}$ and 0.6°C for the wet and dry experiments, respectively.

439 Our study showed significant impacts of soil moisture initial conditions on the surface energy
440 fluxes. For the wet experiments, we found that the cooling of surface temperature is associated
441 with a decrease of the sensible heat flux, an increase of the latent heat flux and a decrease of the
442 PBL depth. For the dry experiments, the warming of surface temperature is associated with a
443 increase of the sensible heat flux, a decrease of the latent heat flux and an increase of the PBL
444 depth.

445 This study showed that soil moisture as a boundary condition plays a major role in controlling
446 summer climate variability not only over the Sahel band but also over humid zones such as
447 Guinea Coast. Therefore, the good prescription of soil moisture initial conditions could improve
448 the simulation of precipitation and temperature, which would help to reduce biases in climate
449 model simulations. Overall, land surface initialization can contribute to improving sub-seasonal
450 to seasonal forecast skill, but this requires further investigation. We recognize that

451 This study is the first investigating the impact of soil moisture initial conditions in West Africa.
452 However, this study is based on idealized experiments : sensitivity experiments such as "wet"
453 and "dry" ones conducted in this study were not intended to simulate real climate since such
454 extremes are very rare. Moreover, this study is very specific to RegCM4. In the future, an
455 investigation using different RCMs in a multi-model framework will contribute to better quantify
456 the impact of soil moisture initial conditions. At shorter timescales, there is a need to understand
457 how the soil moisture initial conditions contribute to the triggering and the maintenance of the
458 mesoscale convective systems which are known to explain large amount of rainfall in the region
459 (Mathon et al., 2002). Finally, in the context of climate change, considering the projected
460 increase of high-impact weather events in the region, there is a need to explore the sensitivity of
461 soil moisture initial conditions to climate extremes.

462

463

464 **Authors contributions**

465 The authors declare to have no conflict of interest with this work. B. Koné and A. Diedhiou fixed
466 the analysis framework. B. Koné carried out all the simulations and figures production
467 according to the outline proposed by A. Diedhiou. B. Koné and A. Diedhiou, S. Anquetin and A.
468 Diawara worked on the analyses. All authors contributed to the drafting of this manuscript.

469 **Acknowledgements**

470 The research leading to this publication is co-funded by the NERC/DFID “Future Climate for
471 Africa” programme under the AMMA-2050 project, grant number NE/M019969/1 and by IRD
472 (Institut de Recherche pour le Développement; France) grant number UMR IGE Imputation
473 252RA5.

474

475

476

477

478

479

480

481

482

483

484

485

486

487

488

489

490

491

492

493

494 **References:**

495

496 Beljaars A. C. M., Viterbo P., Miller M. J., and Betts A. K.: The anomalous rainfall over the
497 United States during July 1993: Sensitivity to land surface parameterization and soil moisture
498 anomalies, *Mon. Weather Rev.*, 124(3), 362–382, doi:10.1175/1520-0493(1996)124<0362:
499 TAROTU>2.0.CO;2, 1996.

500

501 Bosilovich, M. G., and Sun W. Y.: Numerical simulations of the 1993 Midwestern flood: Land–
502 atmosphere interactions. *J. Climate*, 12, 1490–1505, 1999.

503

504 Cook K. H.: Generation of the African easterly jet and its role in determining West African
505 precipitation, *J. Climate*, 12, 1165–1184, [https://doi.org/10.1175/1520-0442\(1999\)012](https://doi.org/10.1175/1520-0442(1999)012)
506 <1165:GOTAEJ> 2.0.CO;2, 1999.

507

508 Damien Decremer, Chul E. Chung, Annica M. L. Ekman & Jenny Brandefelt (2014) Which
509 significance test performs the best in climate simulations?, *Tellus A: Dynamic Meteorology and*
510 *Oceanography*, 66:1, DOI: 10.3402/tellusa.v66.23139.

511

512 Danielson J.J., and Gesch D.B.: Global multi-resolution terrain elevation data 2010
513 (GMTED2010): U.S. Geological Survey Open-File Report 2011–1073, 26 p, 2011.

514

515 Dirmeyer P. A., Koster R. D., and Guo Z.: Do global models properly represent the feedback
516 between land and atmosphere, *J. Hydrometeorol.*, 7(6), 1177–1198, doi:10.1175/JHM532.1,
517 2006.

518

519 Douville, F. Chauvin, and H. Broqua.: Influence of soil moisture on the Asian and African
520 monsoons. Part I: Mean monsoon and daily precipitation. *J. Climate*, 14, 2381–2403, 2001.

521

522 Eltahir E. A. B.: A soil moisture-rainfall feedback mechanism 1. Theory and observations, *Water*
523 *Resour. Res.*, 34, 765–776, doi:10.1029/97WR03499, 1998.

524

525 Emanuel K. A.: A scheme for representing cumulus convection in large-scale models. *Journal of*
526 *the Atmospheric Science* 48: 2313–2335, 1991.

527

528 Funk, C., Peterson, P., Landsfeld, M. et al. The climate hazards infrared precipitation with
529 stations—a new environmental record for monitoring extremes. *Sci Data* 2, 150066 (2015).
530 <https://doi.org/10.1038/sdata.2015.66>

531

532 Gao, X.-J., Shi, Y., and Giorgi, F.: Comparison of convective parameterizations in RegCM4
533 experiments over China with CLM as the land surface model, *Atmos. Ocean. Sci. Lett.*, 9, 246–
534 254, <https://doi.org/10.1080/16742834.2016.1172938>, 2016.

535

536 Giorgi F., Coppola E., Solmon F., Mariotti L., Sylla M. B., Bi X., Elguindi N., Diro G. T., Nair
537 V., Giuliani G., Cozzini S., Guettler I., O’Brien T., Tawfik A., Shalaby A., Zakey A. S., Steiner
538 A., Stordal F., Sloan L., and Brankovic C.: RegCM4: model description and preliminary tests
539 over multiple CORDEX domains, *Clim. Res.*, 52, 7–29, <https://doi.org/10.3354/cr01018>, 2012.

540

541 Grell G., Dudhia J. and Stauffer D. R.: A description of the fifth generation Penn State/NCAR
542 Mesoscale Model (MM5), National Center for Atmospheric Research Tech Note NCAR/TN-
543 398+STR, NCAR, Boulder, CO, 1994.

544

545 Harris I., Jones P. D., Osborn T. J. and Lister D. H.: Updated high-resolution grids of monthly
546 climatic observations, *Int. J. Climatol.*, 34, 623–642, <https://doi.org/10.1002/joc.3711>, 2013.

547

548 Holtslag A., De Bruijn E., and Pan H. L.: A high resolution air mass transformation model for
549 short-range weather forecasting, *Mon. Weather Rev.*, 118, 1561–1575, 1990.

550

551 Hong S-Y. and Pan H-L.: Impact of soil moisture anomalies on seasonal, summertime
552 circulation over North America in a regional climate model. *J. Geophys. Res.*, 105 (D24), 29
553 625–29 634, 2000.

554

555 Jaeger E. B., and Seneviratne S.I.: Impact of soil moisture-atmosphere coupling on European
556 climate extremes and trends in a regional climate model, *Clim. Dyn.*, 36(9-10), 1919-1939,
557 doi:10.1007/s00382-010-0780-8, 2011.

558

559 Kang S, Im E.-S. and Ahn J.-B.: The impact of two land-surface schemes on the characteristics
560 of summer precipitation over East Asia from the RegCM4 simulations *Int. J. Climatol.* 34: 3986-
561 3997, 2014.

562

563 Kiehl J., Hack J., Bonan G., Boville B., Breigleb B., Williamson D., Rasch P.; Description of the
564 NCAR Community Climate Model (CCM3). National Center for Atmospheric Research Tech
565 Note NCAR/TN-420+STR, NCAR, Boulder, CO, 1996.

566

567 Kim J-E., and Hong S-Y.: Impact of Soil Moisture Anomalies on Summer Rainfall over East
568 Asia: A Regional Climate Model Study, *Journal of Climate*. Vol. 20, 5732–5743, DOI:
569 10.1175/2006JCLI1358.1, 2006.

570

571 Kirtman B.P., Schopf P. S.: Decadal Variability in ENSO Predictability and Prediction. *Journal*
572 *of Clim.* 11, 2804, 1998.

573

574 Koné B., Diedhiou A., N’datchoh E. T., Sylla M. B., Giorgi F., Anquetin S., Bamba A., Diawara
575 A., and Koba A. T.: Sensitivity study of the regional climate model RegCM4 to different
576 convective schemes over West Africa. *Earth Syst. Dynam.*, 9, 1261–1278.
577 <https://doi.org/10.5194/esd-9-1261-2018>, 2018.

578

579 Koster R. D., Dirmeyer P. A., Zhichang G., Bonan G., Chan E., Cox P., Gordon C. T., Kanae S.,
580 Kowalczyk E., Lawrence D., Liu P., Lu C. H, Malyshev S., McAvaney B., Mitchell K, Mocko
581 D., Oki T., Oleson K., Pitman A., Sud Y. C., Taylor C. M., Verseghy D., Vasic R., Xue Y.,
582 Yamada T.: Regions of strong coupling between soil moisture and precipitation, *Science*, 305,
583 1138–1140, doi:10.1126/science.1100217, 2004.

584

585 Lawrence D.M., Oleson K.W., Flanner M.G., Thornton P.E., Swenson S.C., Lawrence P.J., Zeng
586 X., Yang Z.-L., Levis S., Sakaguchi K., Bonan G.B., and Slater A.G.:Parameterization
587 improvements and functional and structuraladvances in version 4 of the Community Land
588 Model. *J. Adv. Model. Earth Sys.* 3. DOI:10.1029/2011MS000045, 2011.

589
590 Liu D., Wang G. L., Mei R., Yu Z. B. and Gu H. H.: Diagnosing the strength of land-atmosphere
591 coupling at sub-seasonal to seasonal time scales in Asia, *J. Hydrometeor.*, doi:10.1175/JHM-D-
592 13-0104.1, 2013.

593
594 Liu D., Wang R. Mei Z. Yu, and Yu M.: Impact of soil moisture initial conditions anomalies
595 on climate mean and extremes over Asia, *J. Geophys. Res. Atmos.*, 119, 529–545,
596 doi:10.1002/2013JD020890, 2014.

597
598 Loveland, T. R., Reed, B. C., Brown, J. F., Ohlen, D. O., Zhu, J., Yang, L., and Merchant, J. W.:
599 Development of a global land cover characteristics database and IGBP DISCover from 1-km
600 AVHRR Data, *Int. J. Remote. Sens.*, 21, 1303–1330, 2000.

601
602 Mathon, V., Diedhiou, A., & Laurent, H. (2002). Relationship between easterly waves and
603 mesoscale convective systems over the Sahel. *Geophysical research letters*, 29(8), 57-1.

604
605 Menéndez, C. G., Giles, J., Ruscica, R., Zaninelli, P., Coronato, T., Falco, M., ... & Li, L. (2019).
606 Temperature variability and soil–atmosphere interaction in South America simulated by two
607 regional climate models. *Climate Dynamics*, 53(5), 2919-2930.

608
609 Oglesby R. J., and Erickson III D. J.: Soil moisture and the persistence of North American
610 drought. *J. Climate*, 2, 1362–1380, 1989.

611
612 Oglesby R. J., Marshall S., Erickson III D. J., Roads J. O. and Robertson F. R.: Thresholds in
613 atmosphere-soil moisture interactions: Results from climate model studies. *J. Geophys. Res.*, 107,
614 4244, doi:10.1029/2001JD001045, 2002.

615
616 Oleson K., Lawrence D. M., Bonan G. B., Drewniak B., Huang M., Koven C. D., Yang Z. -L.:
617 Technical description of version 4.5 of the Community Land Model (CLM) (No. NCAR/TN-
618 503+STR). doi:10.5065/D6RR1W7M, 2013.

619
620 Paeth H., Girmes R., Menz G. and Hense A.: Improving seasonal forecasting in the low latitudes,
621 *Mon. Weather Rev.*, 134, 1859-1879, 2006.

622

623 Pal J. S., Small E. E. and Elthair E. A.: Simulation of regional scale water and energy budgets:
624 representation of subgrid cloud and precipitation processes within RegCM, *J. Geophys. Res.*,
625 105, 29579–29594, 2000.

626

627 Pal J. S. and Eltahir E. A. B.: Pathways relating soil moisture conditions to future summer
628 rainfall within a model of the land–atmosphere system. *J. Climate*, 14, 1227–1242, 2001.

629

630 Peterson T. C., Folland C., Gruza G., Hogg W. Mokssit A., Plummer N.: Report on the activities
631 of the working group on climate change detection and related rapporteurs 1998-2001. Geneva
632 (Switzerland): WMO Rep. WCDMP 47, WMO-TD 1071, 2001.

633

634 Nicholson S. E.: The West African Sahel: a review of recent studies on the rainfall regime and its
635 interannual variability, *Meteorology*, 453521, 32 p., <https://doi.org/10.1155/2013/453521>, 2013.

636 Nikulin G., Jones C., Samuelsson P., Giorgi F., Asrar G., Büchner M., Cerezo-Mota R.,
637 Christensen O. B., Déque M., Fernandez J., Hansler A., van Meijgaard E., Sylla M. B. and
638 Sushama L.: Precipitation climatology in an ensemble of CORDEX-Africa regional climate
639 simulations, *J. Climate*, 6057–6078, <https://doi.org/10.1175/JCLI-D-11-00375.1>, 2012.

640

641 Rasmusson E. M. and Carpenter T. H.: Variations in Tropical Sea Surface Temperature and
642 Surface Wind Fields Associated with the Southern Oscillation/El Niño. *Mon. Weather Rev.* 110,
643 354, 1982.

644

645 Reynolds, R. W. and Smith, T. M.: Improved global sea surface temperature analysis using
646 optimum interpolation, *J. Climate*, 7, 929–948, 1994.

647

648 Seager R., and Vecchi G. A.: Greenhouse warming and the 21st century hydroclimate of
649 southwestern North America. *Proc. Natl. Acad. Sci. USA*, 107, 21 277–21 282,
650 [doi:10.1073/pnas.0910856107](https://doi.org/10.1073/pnas.0910856107), 2010.

651

652 Simmons A. S., Uppala D. D. and Kobayashi S.: ERA-interim: new ECMWF reanalysis products
653 from 1989 onwards, *ECMWF Newsl.*, 110, 29–35, 2007.

654

655 Solmon F., Giorgi F., and Liousse C.: Aerosol modeling for regional climate studies: application
656 to anthropogenic particles and evaluation over a European/African domain, *Tellus B*, 58, 51–72,
657 2006.

658

659 Sundqvist H. E., Berge E., and Kristjansson J. E.: The effects of domain choice on summer
660 precipitation simulation and sensitivity in a regional climate model, *J. Climate*, 11, 2698-2712,
661 1989.

662

663 Takahashi, H. G., & Polcher, J. (2019). Weakening of rainfall intensity on wet soils over the wet
664 Asian monsoon region using a high-resolution regional climate model. *Progress in Earth and*
665 *Planetary Science*, 6(1), 1-18.

666

667 Thorncroft, C. D. and Blackburn, M.: Maintenance of the African easterly jet, *Q. J. R. Meteorol*
668 *Soc.*, 125, 763–786, 1999.

669

670 Uppala S., Dee D., Kobayashi S., Berrisford P. and Simmons A.: Towards a climate data
671 assimilation system: status update of ERA-interim, *ECMWF Newsl.*, 15, 12–18, 2008.

672

673 Vinnikov K. Y. and Yesserkepova I. B.: Soil moisture: Empirical data and model results, *J. Clim.*,
674 4(1), 66–79, doi:10.1175/1520-0442(1991)004<0066:SMEDAM>2.0.CO;2, 1991.

675

676 Vinnikov K. Y., Robock A., Speranskaya N. A. and Schlosser A.: Scales of temporal and spatial
677 variability of midlatitude soil moisture, *J. Geophys. Res.*, 101(D3), 7163–7174,
678 doi:10.1029/95JD02753, 1996.

679

680 Wang, G., Yu, M., Pal, J. S., Mei, R., Bonan, G. B., Levis, S., and Thornton, P. E.: On the
681 development of a coupled regional climate vegetation model RCM-CLM-CN-DV and its
682 validation its tropical Africa, *Clim. Dynam*, 46, 515–539, 2016.

683

684 Xue Y., De Sales F., Lau K. M. W., Bonne A., Feng J., Dirmeyer P., Guo Z., Kim K. M., Kitoh
685 A., Kumar V., Pocard-Leclercq I., Mahowald N., Moufouma-Okia W., Pegion P., Rowell D. P.,
686 Schemm J., Schulbert S., Sealy A., Thiaw W. M., Vintzileos A., Williams S. F. and Wu M. L.:
687 Intercomparison of West African Monsoon and its variability in the West African Monsoon

688 Modelling Evaluation Project (WAMME) first model Intercomparison experiment, *Clim.*
 689 *Dynam.*, 35, 3–27, <https://doi.org/10.1007/s00382-010-0778-2>, 2010.

690
 691 Zakey A. S., Solmon F., and Giorgi F.: Implementation and testing of a desert dust module in a
 692 regional climate model, *Atmos. Chem. Phys.*, 6, 4687–4704, [https://doi.org/10.5194/acp-6-4687-](https://doi.org/10.5194/acp-6-4687-2006)
 693 2006, 2006.

694
 695 Zeng X., Zhao M. and Dickinson R. E.: Intercomparison of bulk aerodynamic algorithms for the
 696 computation of sea surface fluxes using TOGA COARE and TAO DATA, *J. Climate*, 11, 2628-
 697 2644, 1998.

698 Zhang, J., W.-C. Wang, and J. Wei, Assessing land-atmosphere coupling using soil moisture
 699 from the Global Land Data Assimilation System and observational precipitation, *J. Geophys.*
 700 *Res.*, 113, D17119, doi:10.1029/2008JD009807, 2008.

701 Zhang, J., W.-C. Wang, and L. R. Leung.: Contribution of land-atmosphere coupling to summer
 702 climate variability over the contiguous United States, *J. Geophys. Res.*, 113, D22109,
 703 doi:10.1029/2008JD010136, 2008.

704
 705 Zhang, J. Y., L. Y. Wu, and W. Dong,: Land-atmosphere coupling and summer climate
 706 variability over East Asia, *J. Geophys. Res.*, 116, D05117, doi 10.1029/2010JD014714, 2011.

708 **Tables and figures:**

709

	Central Sahel		West Sahel		Guinea		West Africa	
	PCC	MB (%)	PCC	MB (%)	PCC	MB (%)	PCC	MB (%)
CTRL_2003	0.98	-47.97	0.87	-75.76	0.82	-47.12	0.73	-49.31
CTRL_2004	0.98	-47.89	0.87	-68.35	0.85	-51.97	0.77	-50.56

710

711 **Table1:** The pattern correlation coefficient (PCC) and the mean bias (MB) for JJAS precipitation
712 for model simulations with respect to CHIRPS, calculated for Guinea coast, central Sahel, west
713 Sahel and the entire West African domain during the period 2003 and 2004.

714

715

716

717

718

719

720

721

722

723

724

725

726

727

728

729

730

731

732

733

734

		Central Sahel		West Sahel		Guinea coast		West Africa	
		Δ WC	Δ DC	Δ WC	Δ DC	Δ WC	Δ DC	Δ WC	Δ DC
Precipitation (%)	2003	13.80	-4.09	29.95	6.58	19.40	9.20	8.88	4.68
	2004	15.86	-3.29	38.58	-1.25	26.6	12.68	10.72	7.64
Temperature mean (°C)	2003	-1.48	0.56	-1.55	-0.41	-0.15	0.54	-0.62	0.50
	2004	-1.51	0.47	-1.15	-0.24	-0.19	0.59	-0.41	0.59
Sensible heat (w.m ⁻²)	2003	-16.89	8.57	-39.66	5.31	-2.41	7.52	-14.32	8.06
	2004	-19.53	7.55	-31.97	7.23	-3.01	9.18	-14.46	6.81
Latent heat (w.m ⁻²)	2003	21.27	-6.67	34.21	-6.06	3.09	-13.38	15.86	-8.07
	2004	28.55	-4.81	36.49	-6.20	7.09	-14.64	19.68	-8.53
Bowen ratio	2003	-0.42	0.31	-3.01	-0.05	-0.03	0.12	-0.48	0.28
	2004	-0.64	0.39	-2.49	0.41	-0.64	0.15	-0.57	0.26
PBL (m)	2003	-233.49	81.23	-293.23	-0.16	-94.42	132.74	-128.90	75.57
	2004	-223.06	49.48	-247.08	19.87	-119.38	146.80	-117.69	56.53

735

736 **Table2:** Table summarizing the maximum values of change obtained from the PDF distribution
737 for precipitation, temperature, sensible heat, latent heat, Bowen ratio and PBL, calculated for
738 Guinea coast, central Sahel, west Sahel and the entire West African domain during the period
739 JJAS 2003 and JJAS 2004.

740

741

	Central Sahel		West Sahel		Guinea		West Africa	
	PCC	MB (°C)	PCC	MB (°C)	PCC	MB (°C)	PCC	MB (°C)
CTRL_2003	0.99	1.52	0.99	2.68	0.99	-0.34	0.99	0.85
CTRL_2004	0.99	1.50	0.99	2.14	0.99	-0.57	0.99	0.51

742

743 **Table3:** The pattern correlation coefficient (PCC) and the mean bias (MB) for JJAS 2m-
744 temperature for model simulations with respect to CRU, calculated for Guinea coast, central
745 Sahel, west Sahel and the entire West African domain during the period JJAS 2003 and JJAS
746 2004.

747

748

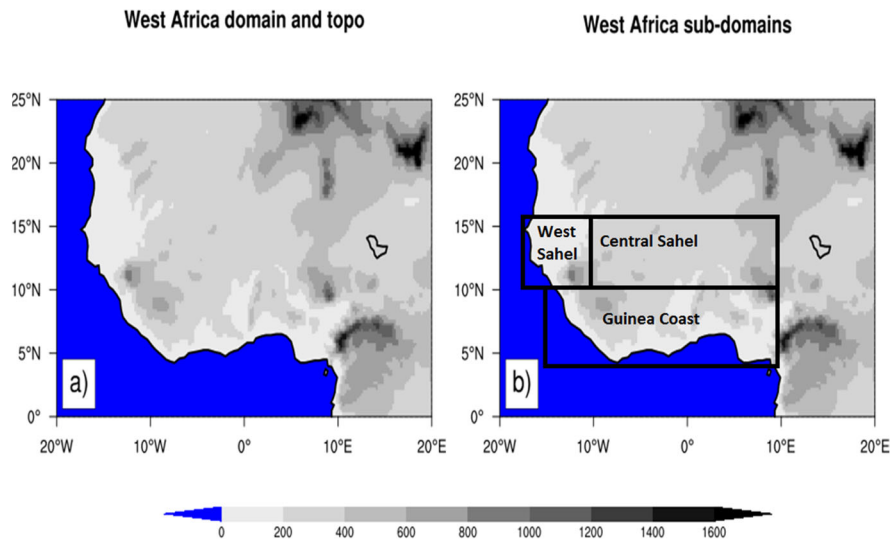
749

750

751

752

753

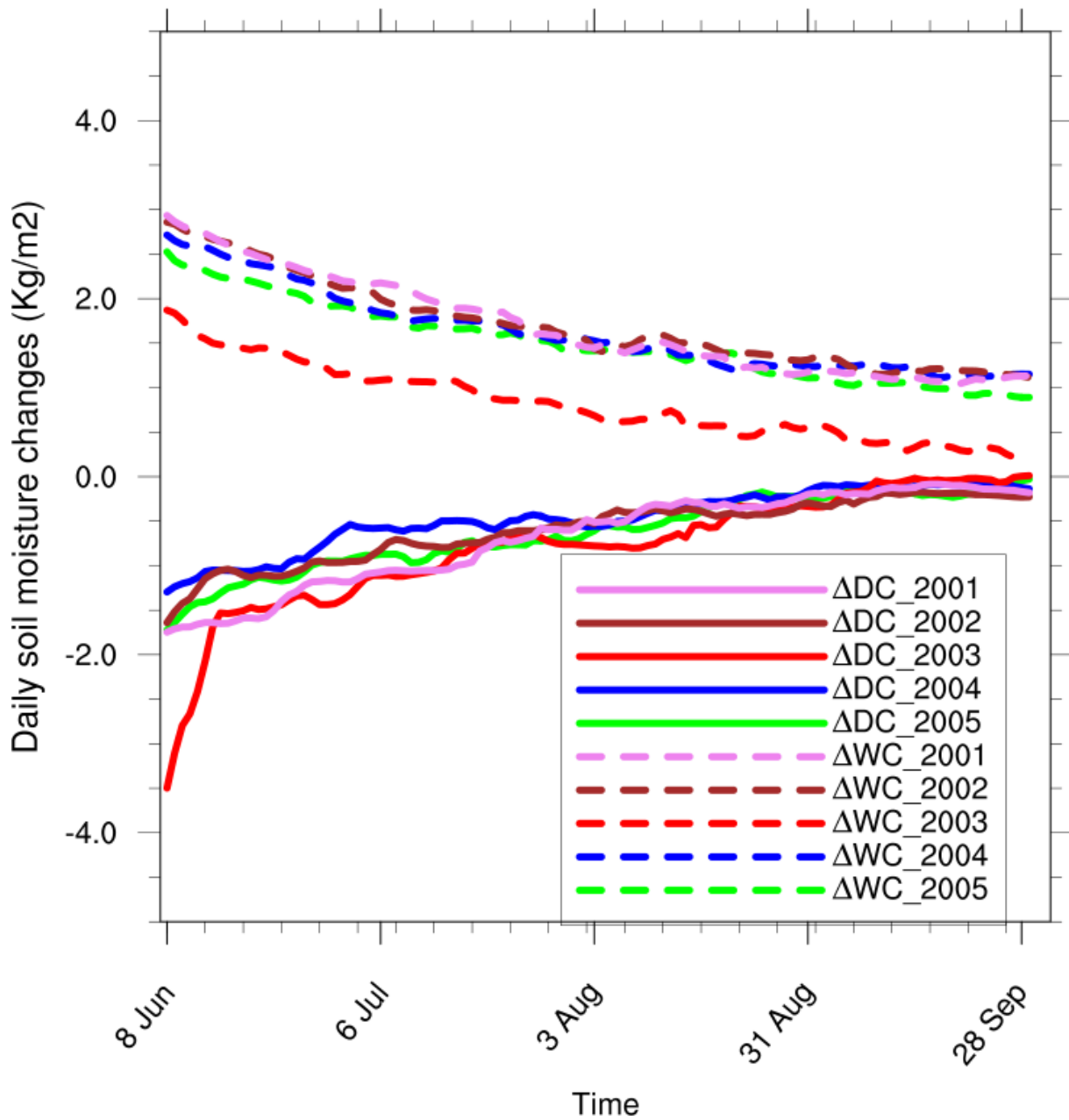


754
755

756 **Figure 1:** Topography of the West African domain. The analysis of the model result has an
757 emphasis on the whole West African domain and the three sub-regions Guinea coast, central
758 Sahel and west Sahel, which are marked with black boxes.

759
760
761
762
763
764
765
766
767
768
769
770
771
772
773
774
775
776
777
778

West Africa



780
 781 **Figure 2:** Changes in daily soil moisture in the 5 runs (JJAS 2001 to 2005) over West African
 782 domain, for the dry (ΔDC) and wet (ΔWC) experiments with respect to their corresponding
 783 control experiment.

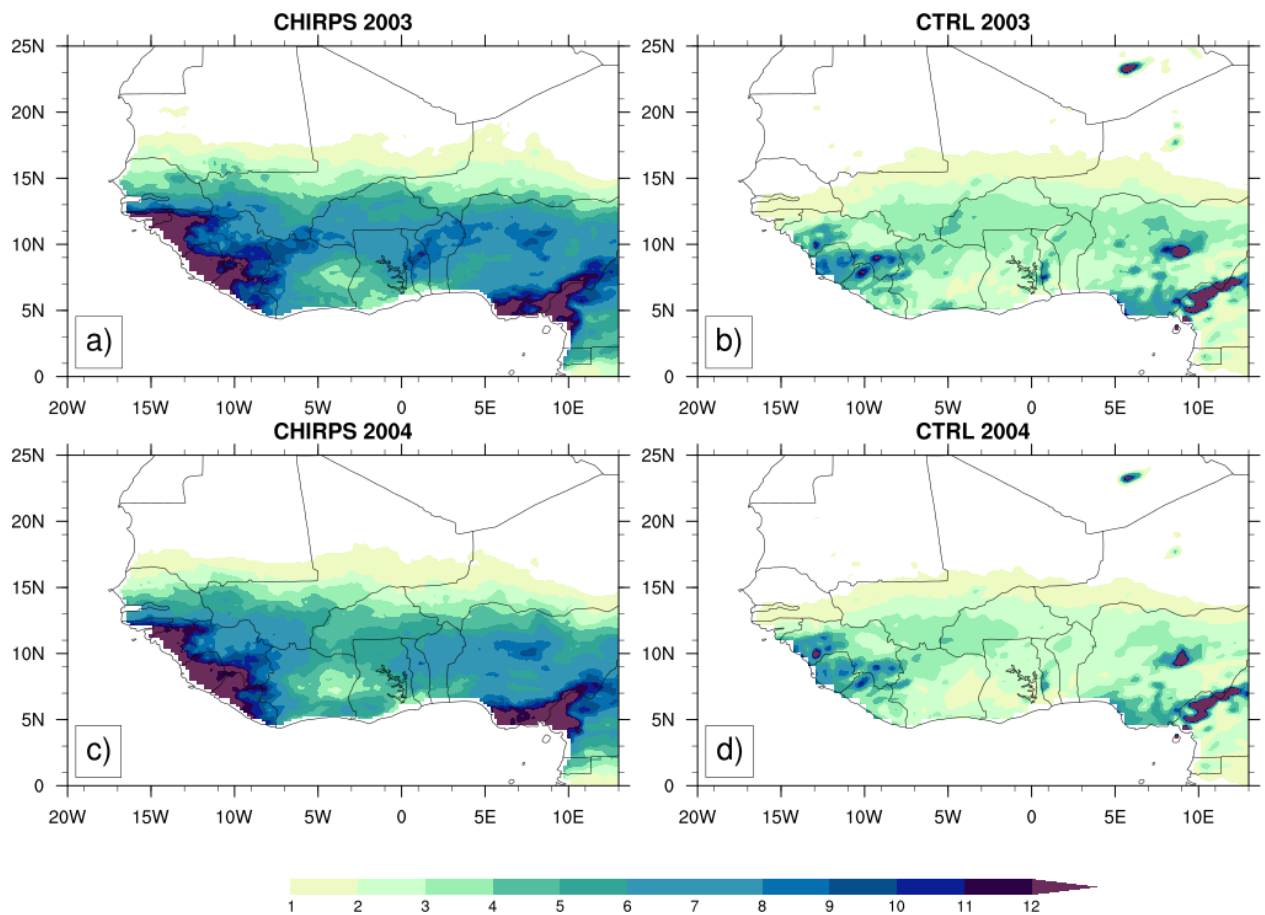
784

785

786

787

788



789
790

791 **Figure3:** Mean precipitation (mm/day) from CHIRPS (a, c) and the simulated control
 792 experiments (CTRL) (b, d) with the reanalysis initial soil moisture ERA20C during JJAS 2003
 793 and JJAS 2004.

794

795

796

797

798

799

800

801

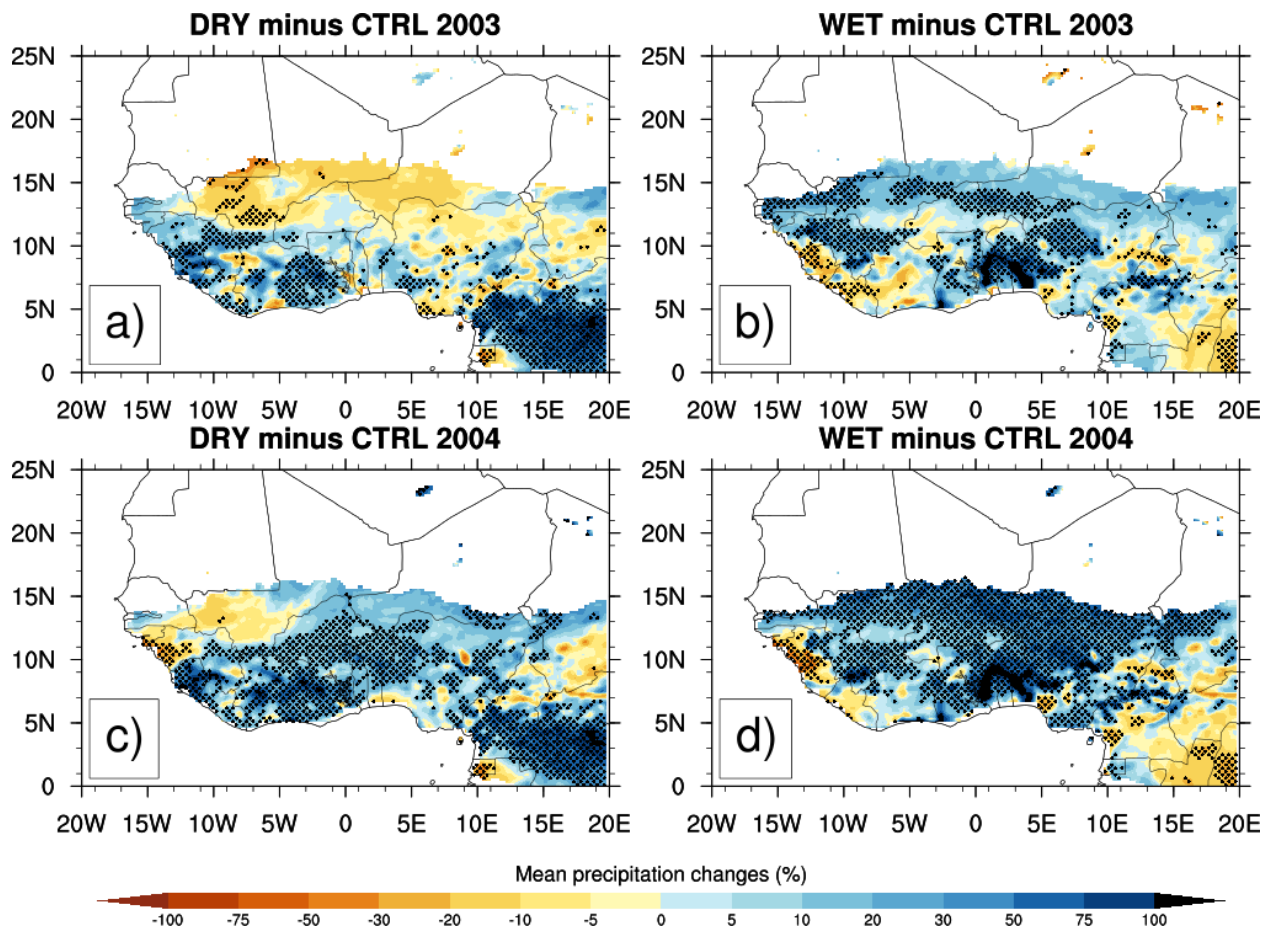
802

803

804

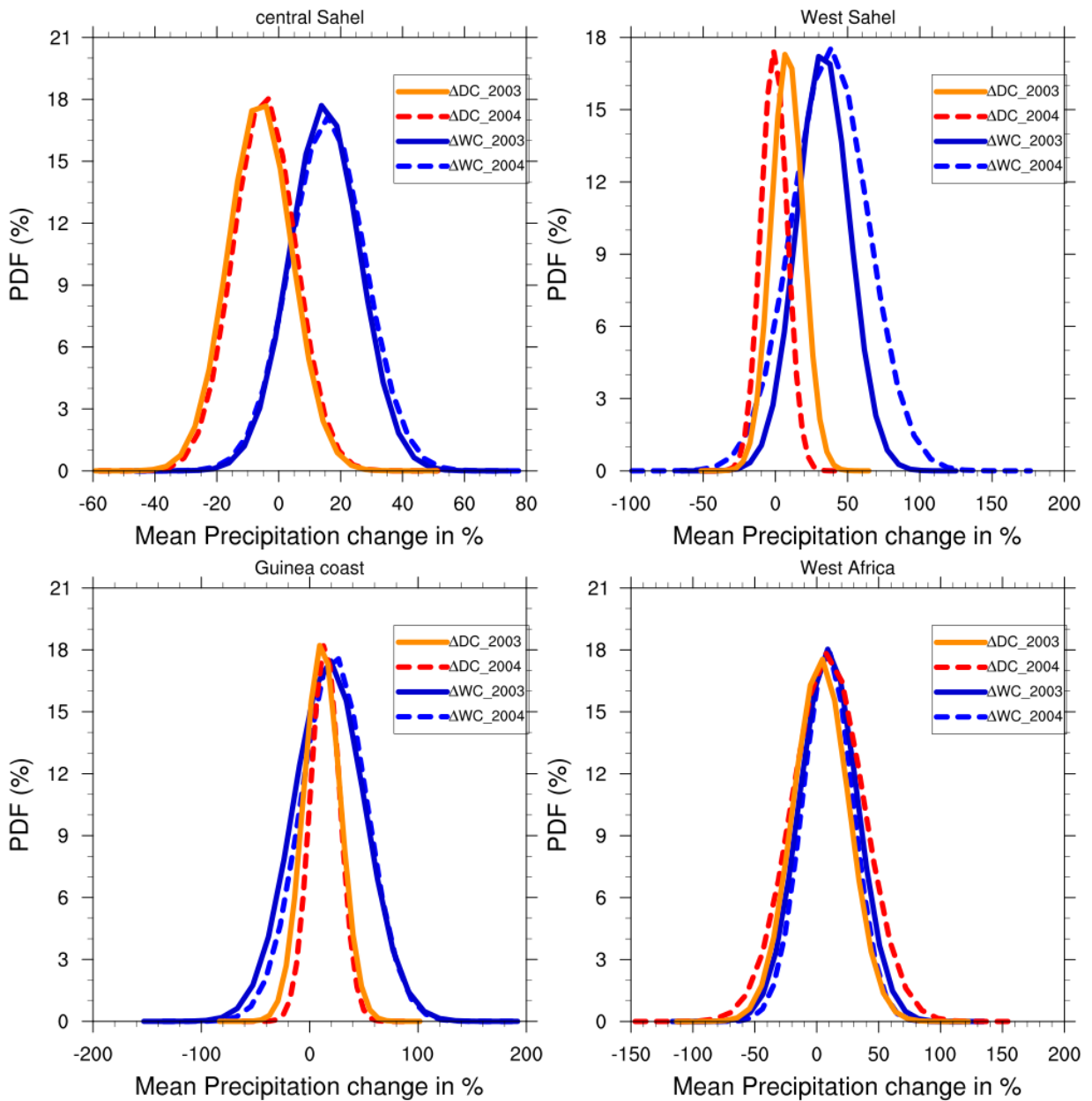
805

806



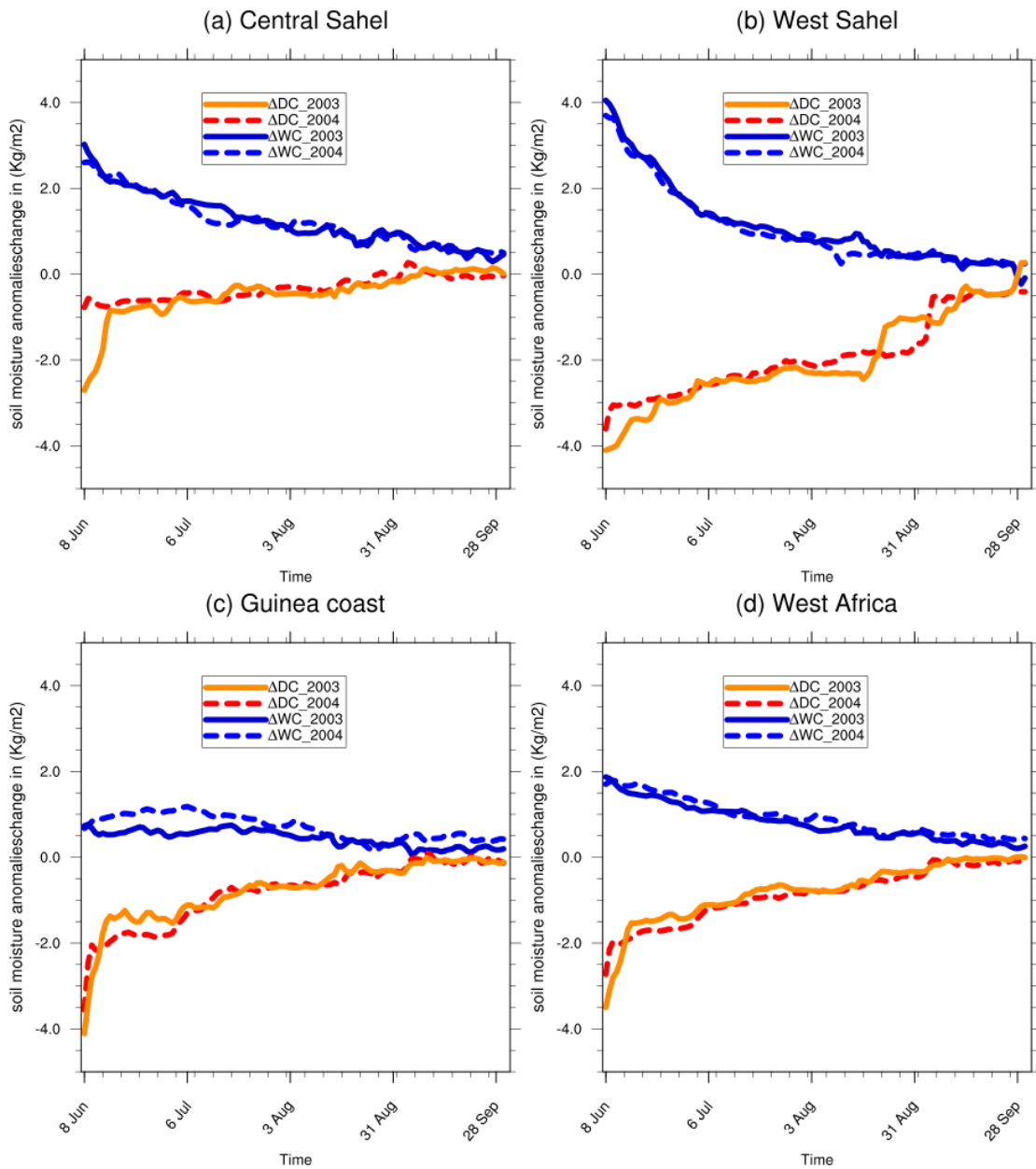
807
 808
 809
 810
 811
 812
 813
 814
 815
 816
 817
 818
 819
 820
 821
 822
 823
 824

Figure4: Changes in mean precipitation (in %) for JJAS 2003 and JJAS 2004, from dry (resp. a and c) and wet (resp. b and d) experiments with respect to the control experiment, the dotted area shows differences that are statistically significant at 0.05 level.



826
 827 **Figure 5:** PDF distributions (%) of mean precipitation changes in JJAS 2003 and JJAS 2004,
 828 over (a) central Sahel, (b) West Sahel, (c) Guinea and (d) West Africa derived from dry (ΔDC)
 829 and wet (ΔWC) experiments compared to the control experiment.

830
 831
 832
 833
 834
 835
 836



838

839 **Figure 6:** Daily domain-average soil moisture changes for JJAS 2003 and JJAS 2004, from dry
 840 (ΔDC) and wet (ΔWC) experiments with respect to the control experiment.

841

842

843

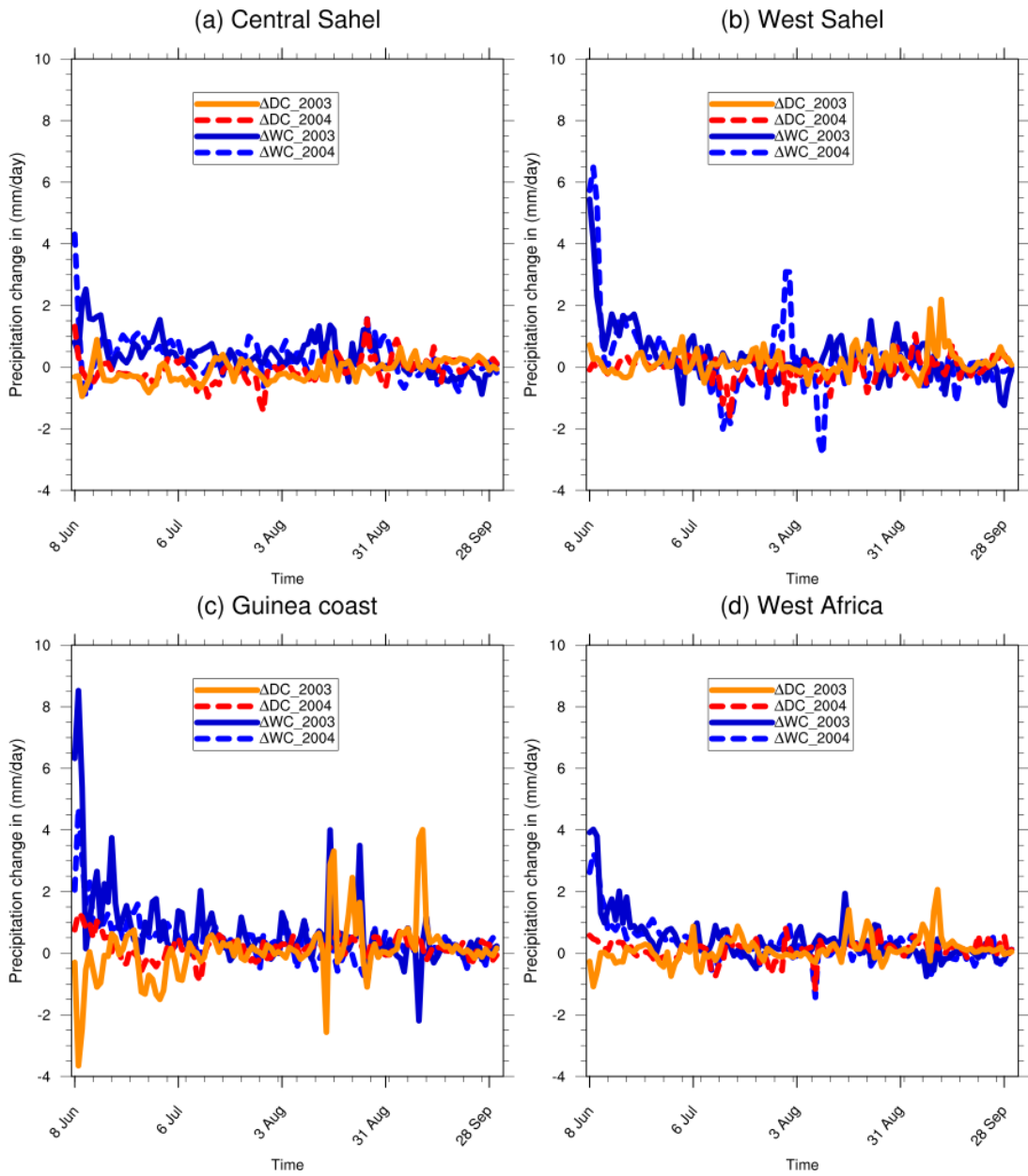
844

845

846

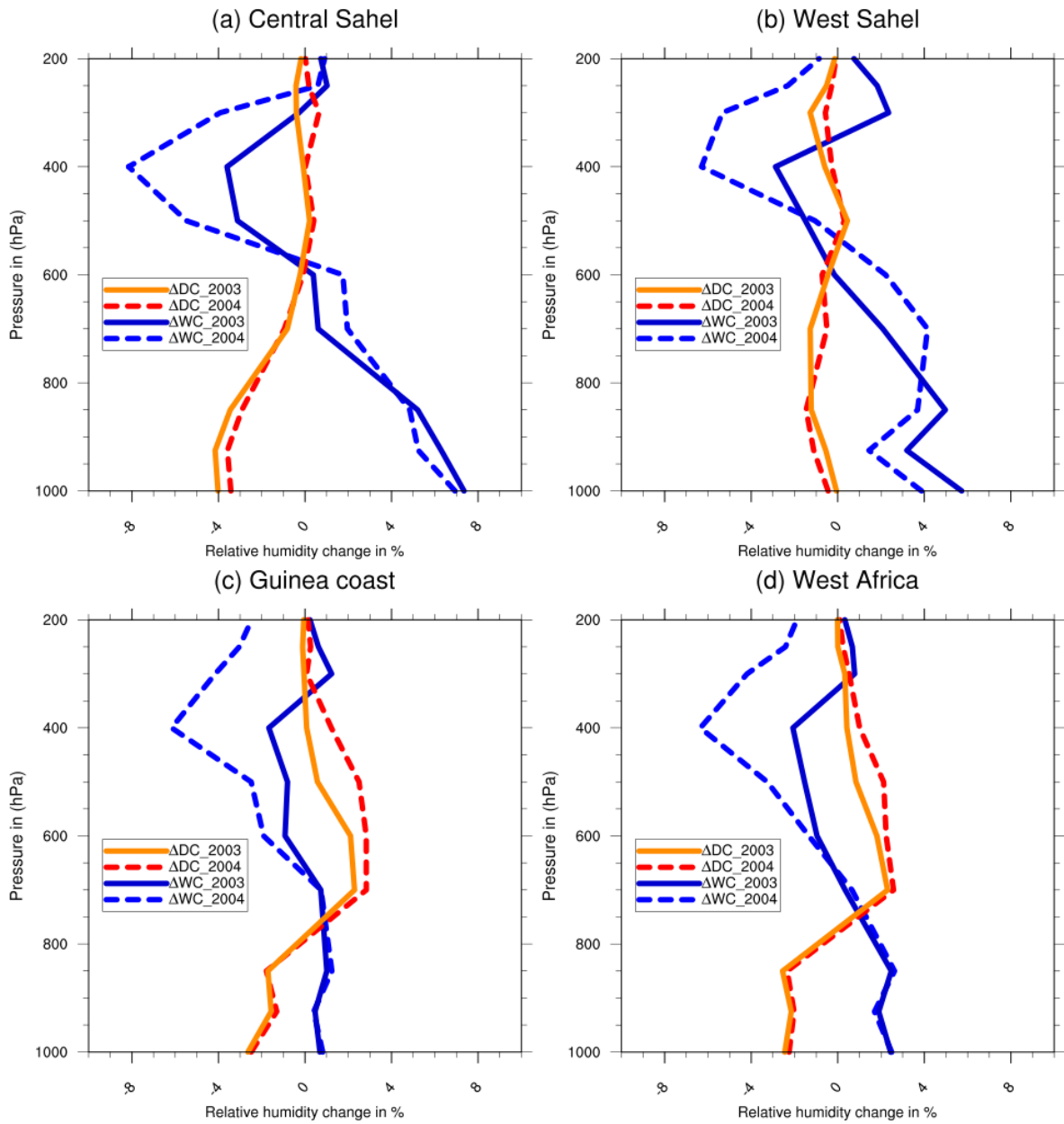
847

848



849
 850
 851
 852 **Figure 7:** Daily domain-average precipitation changes for JJAS 2003 and JJAS 2004, from dry
 853 (ΔDC) and wet (ΔWC) experiments with respect to the control experiment.

854
 855
 856
 857
 858
 859
 860



861

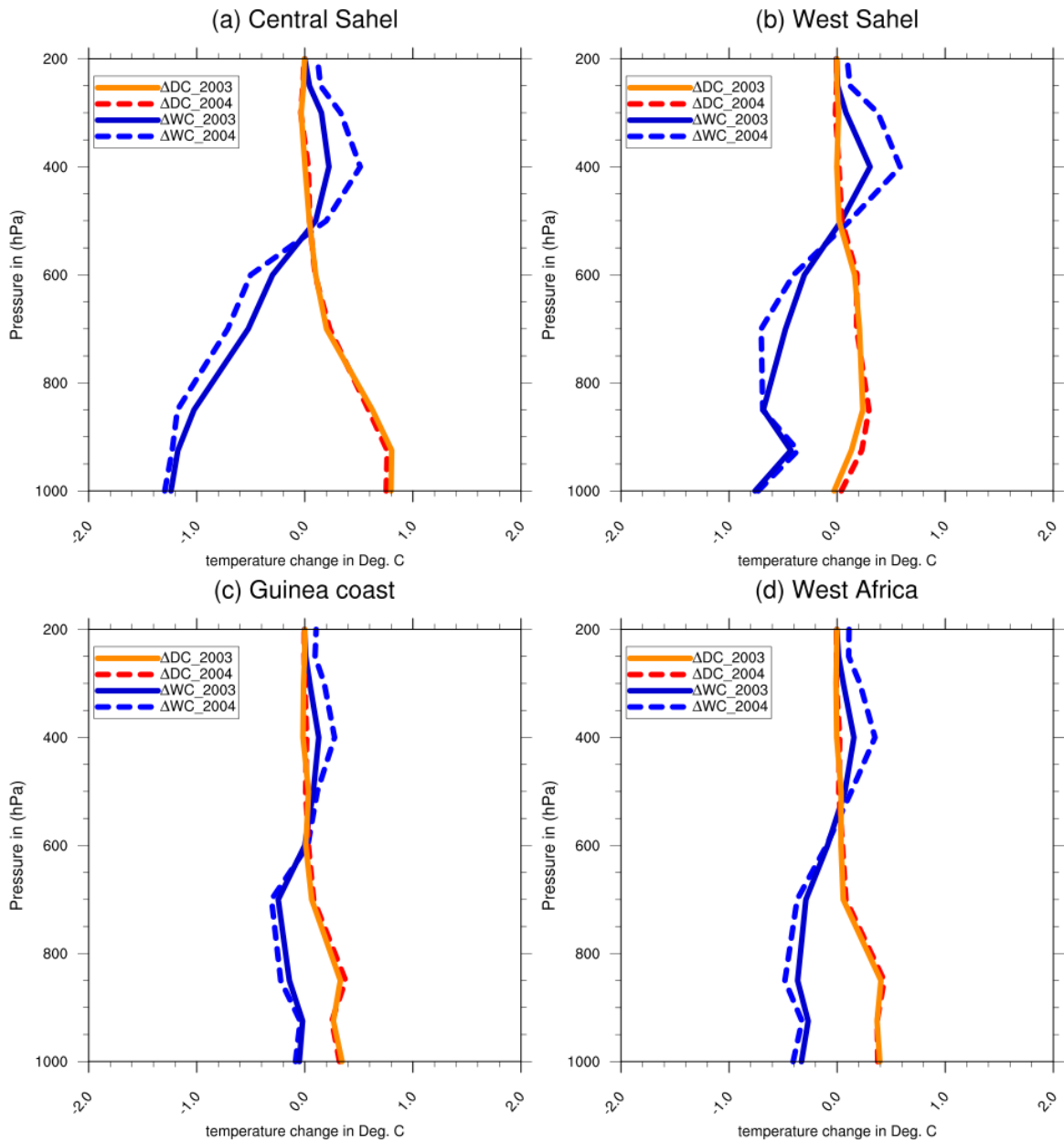
862

863

864 **Figure 8:** Vertical profile changes in Relative humidity for JJAS 2003 and JJAS 2004 from the
 865 dry (ΔDC) and wet (ΔWC) experiments with respect to corresponding control experiment over
 866 (a) central Sahel, (b) west Sahel, (c) Guinea coast, and (d) West Africa.

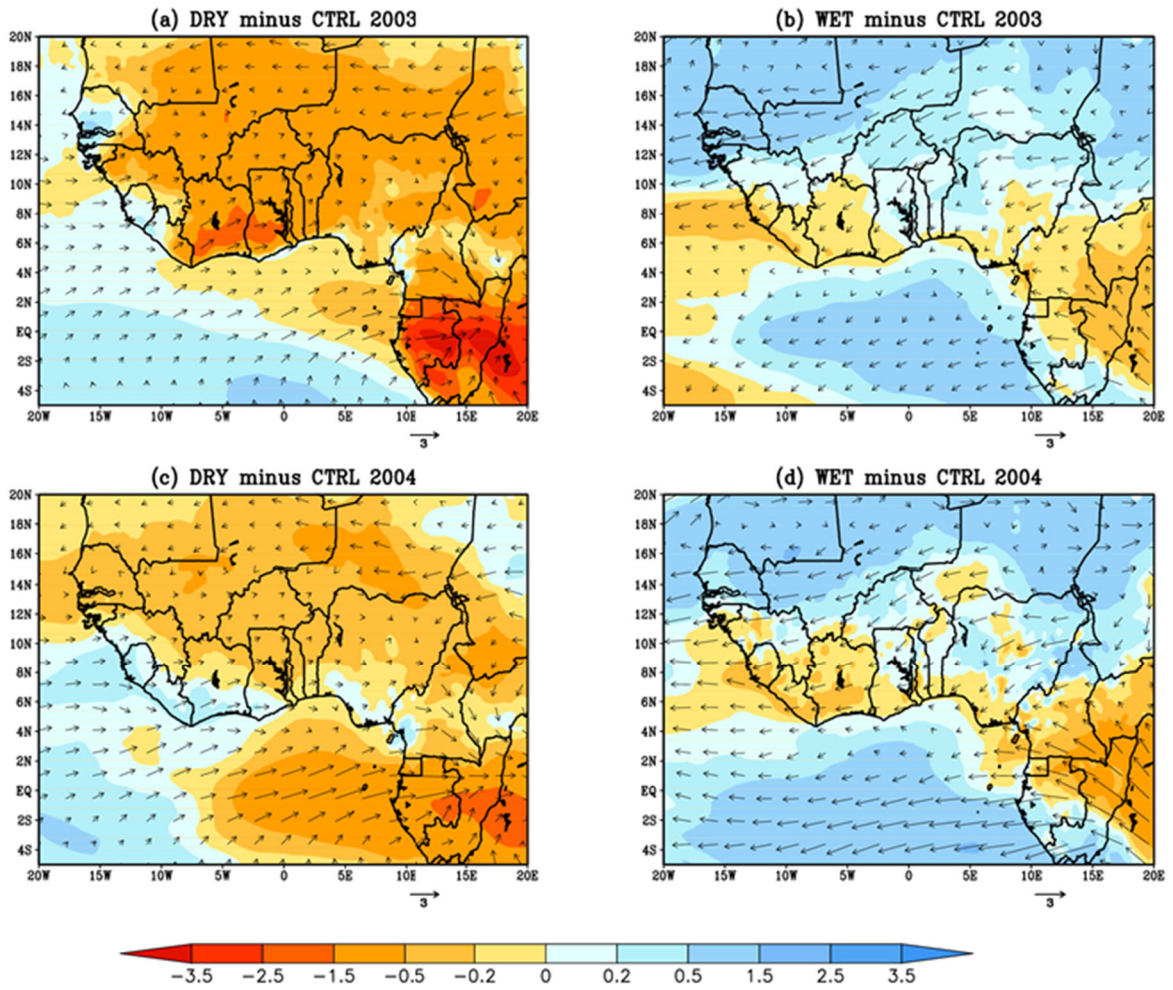
867

868



869
 870 **Figure 9:** Vertical profile changes in temperature for JJAS 2003 and JJAS 2004 from the dry
 871 (ΔDC) and wet (ΔWC) experiments with respect to the control experiment over (a) central Sahel,
 872 (b) west Sahel, (c) Guinea coast, and (d) West Africa.

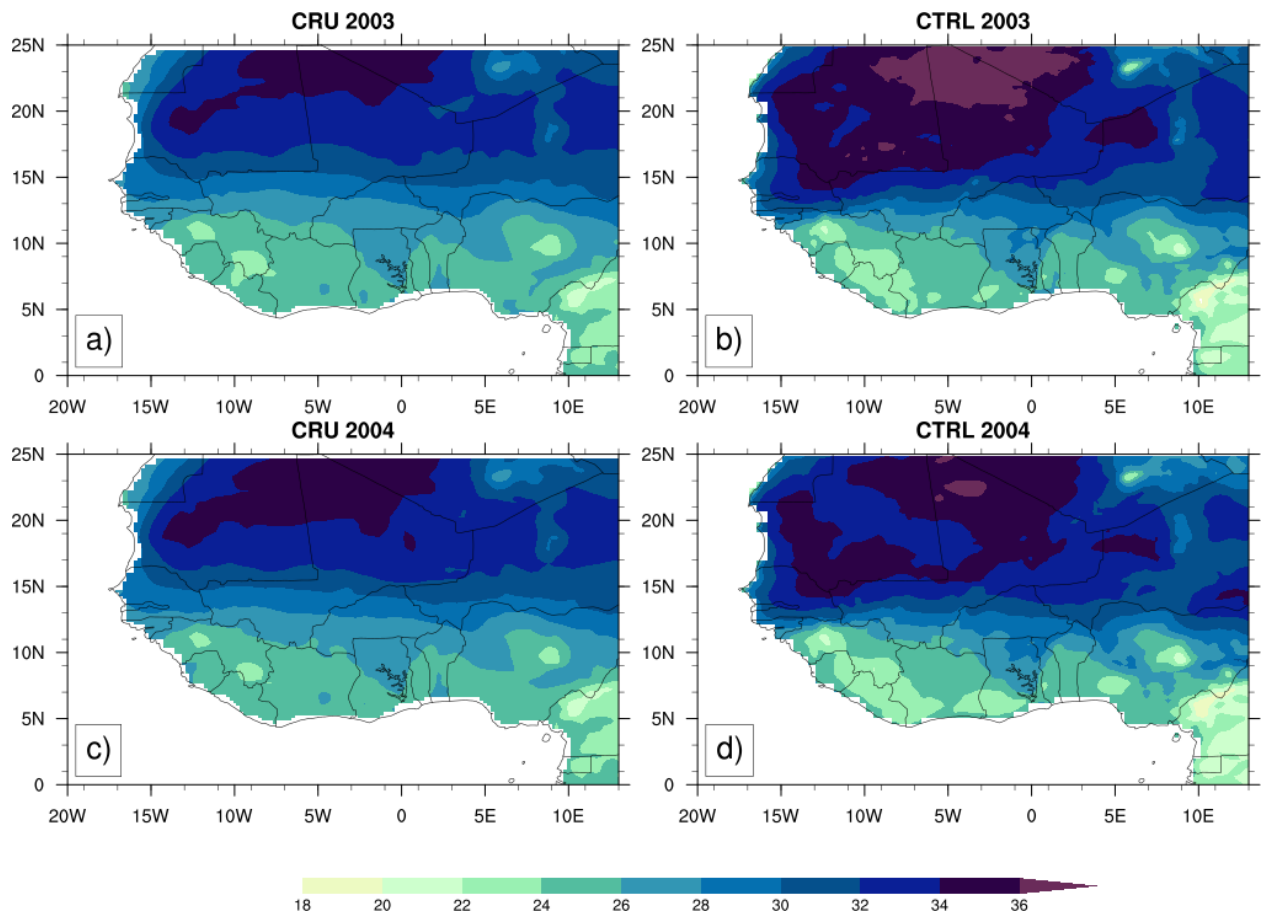
873
 874



875
 876 **Figure 10:** The lower tropospheric wind (850hpa) and moisture bias for JJAS 2003 and JJAS
 877 2004 from the dry (a and c) and wet (b and d) experiments with respect to the control
 878 experiment.

879
 880
 881
 882
 883
 884
 885
 886
 887
 888
 889
 890
 891

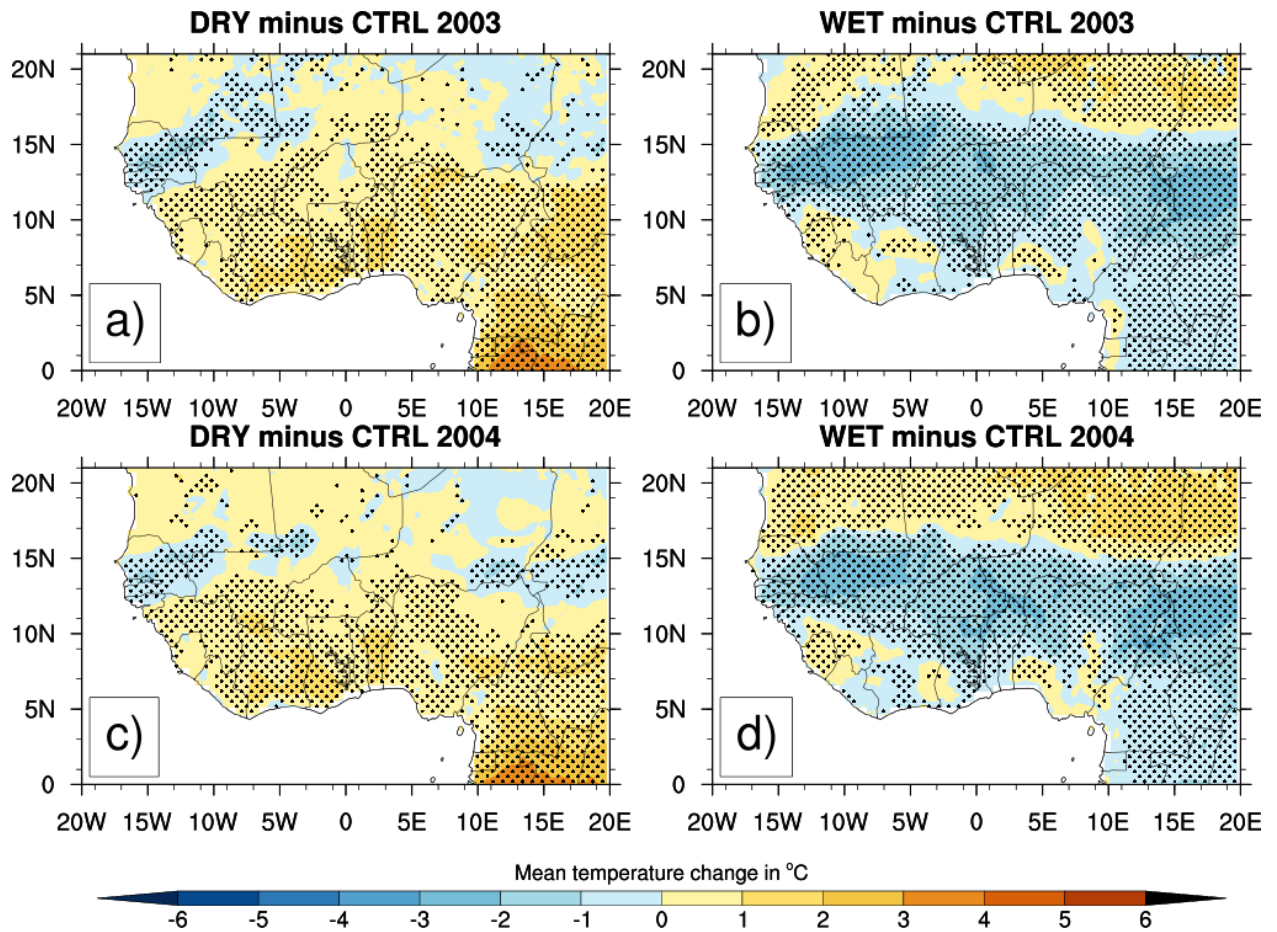
892
893
894



895
896
897
898
899
900
901
902
903
904
905
906
907
908
909

Figure 11: Mean 2m-temperature (°C) from CRU (a and c) for JJAS 2003 and JJAS 2004 and the simulated control experiment (b and d) with the reanalysis initial soil moisture ERA20C.

910
911
912
913

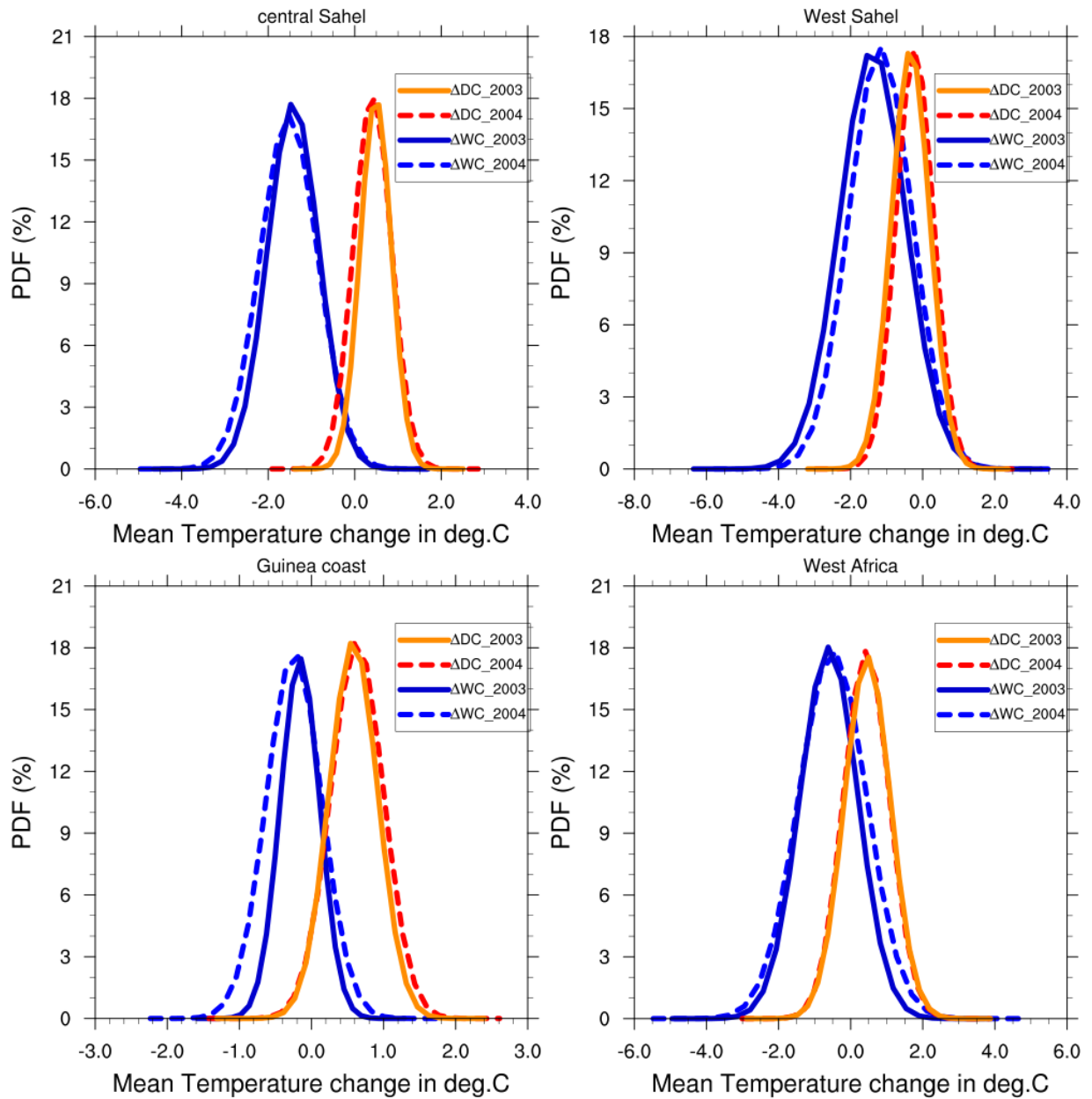


914
915

916 **Figure 12:** Changes in 2m-temperature (°C) for JJAS 2003 and JJAS 2004, from dry (resp. a and
917 c) and wet (resp. b and d) experiments with respect to the control experiment, the dotted area
918 shows differences that are statistically significant at 0.05 level.

919
920
921
922
923
924
925
926
927

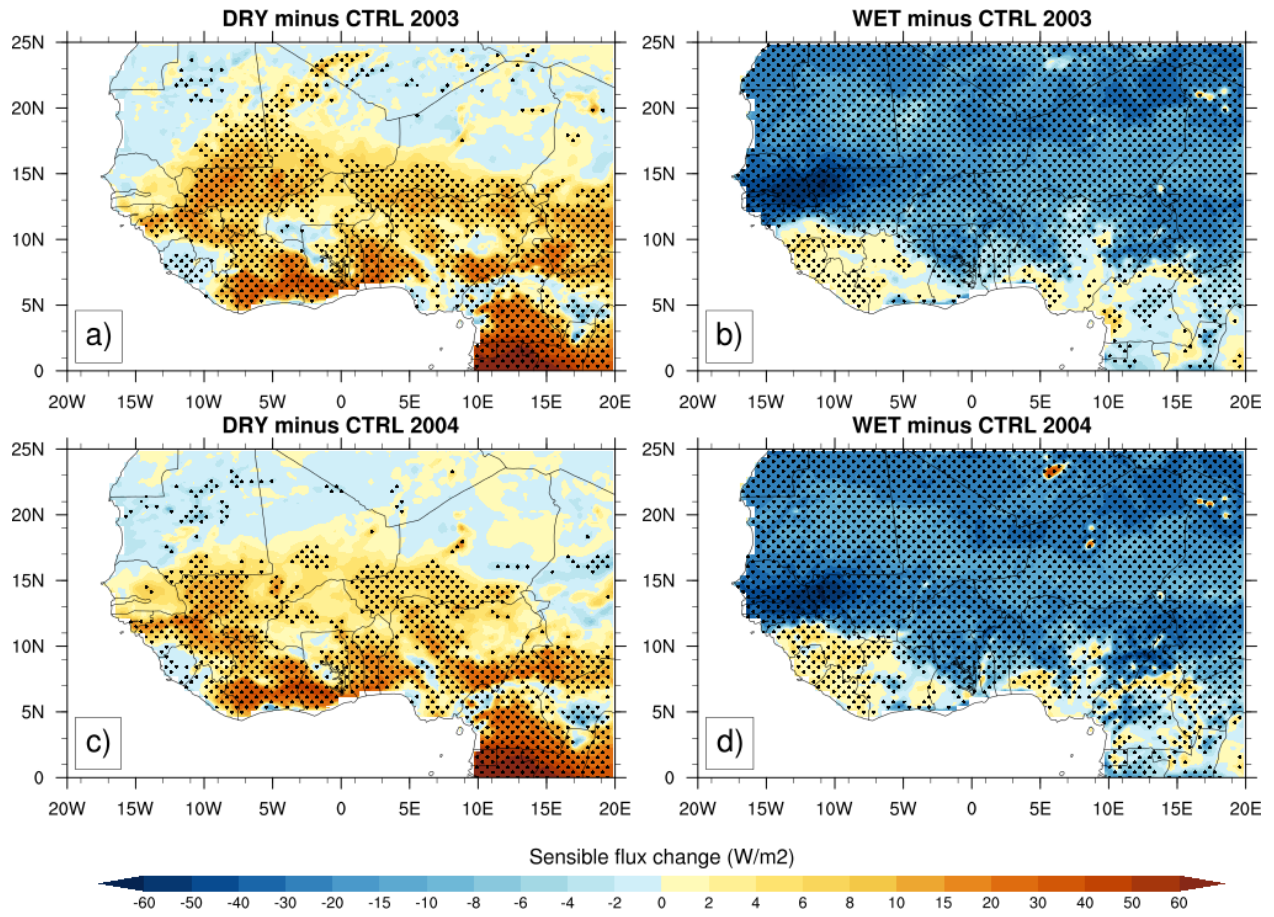
928
929
930
931
932



933
934
935
936
937
938
939

Figure 13: PDF distributions (%) of mean temperature changes in JJAS 2003 and JJAS 2004, over (a) central Sahel , (b) West Sahel, (c) Guinea and (d) West Africa derived from dry (ΔDC) and wet (ΔWC) experiments compared to the control experiment.

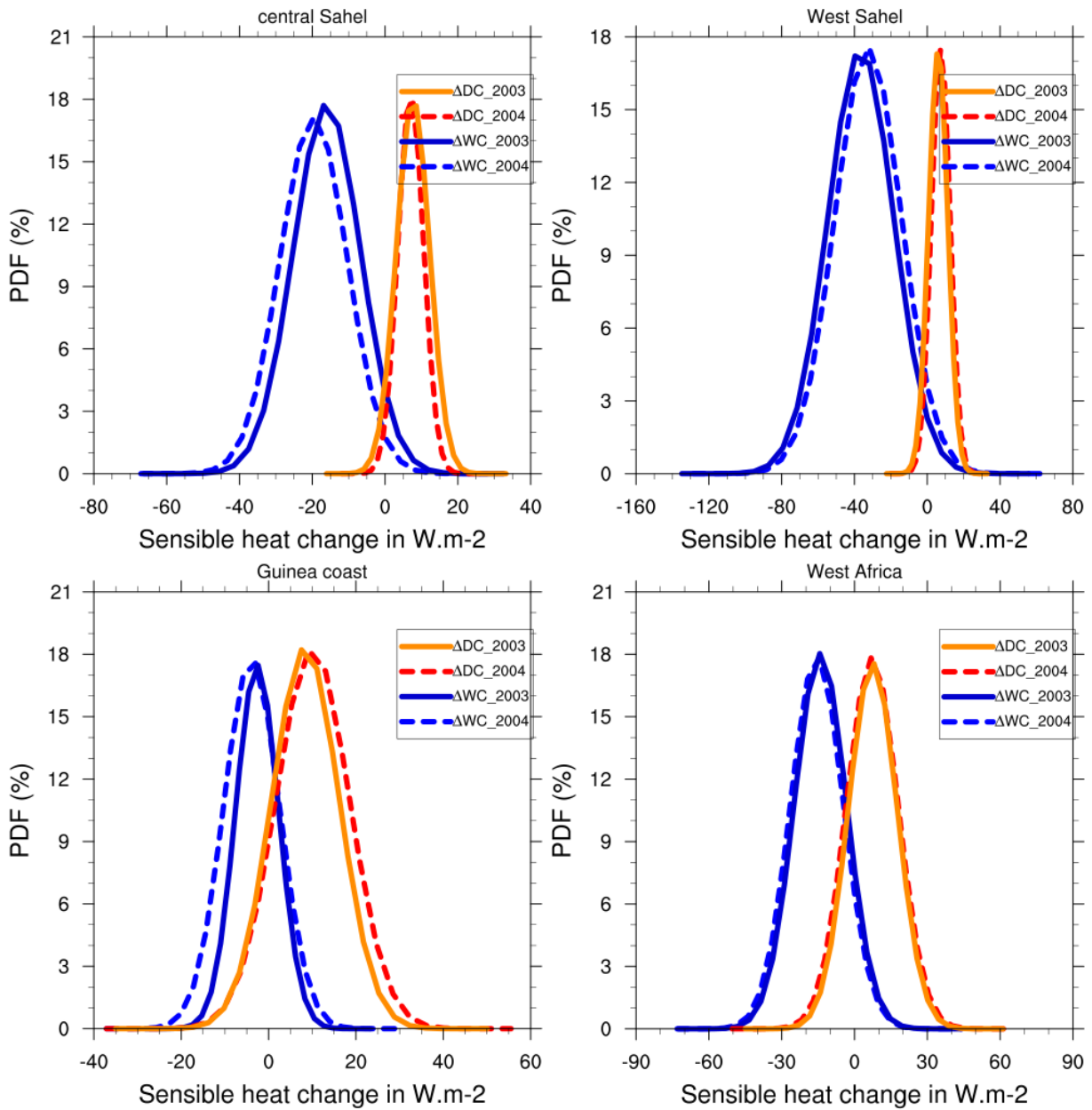
940
941
942
943



944
945
946
947
948
949
950
951
952
953
954
955
956
957

Figure 14: Same as Fig.12 but for sensible heat fluxes (in $W.m^{-2}$).

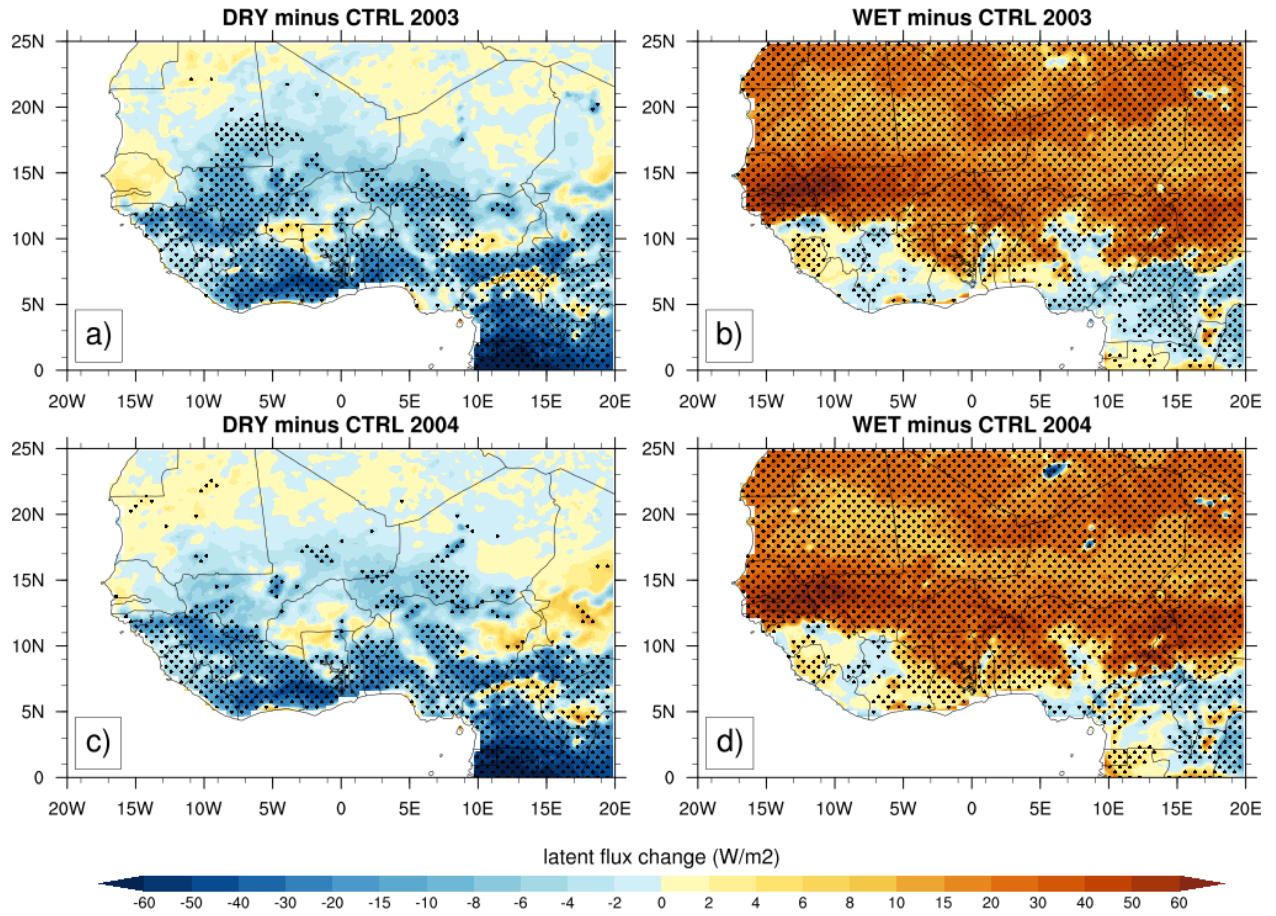
958
959
960
961
962



963
964
965
966
967
968
969

Figure 15: Same as Fig.13 but for sensible heat fluxes (in $W.m^{-2}$).

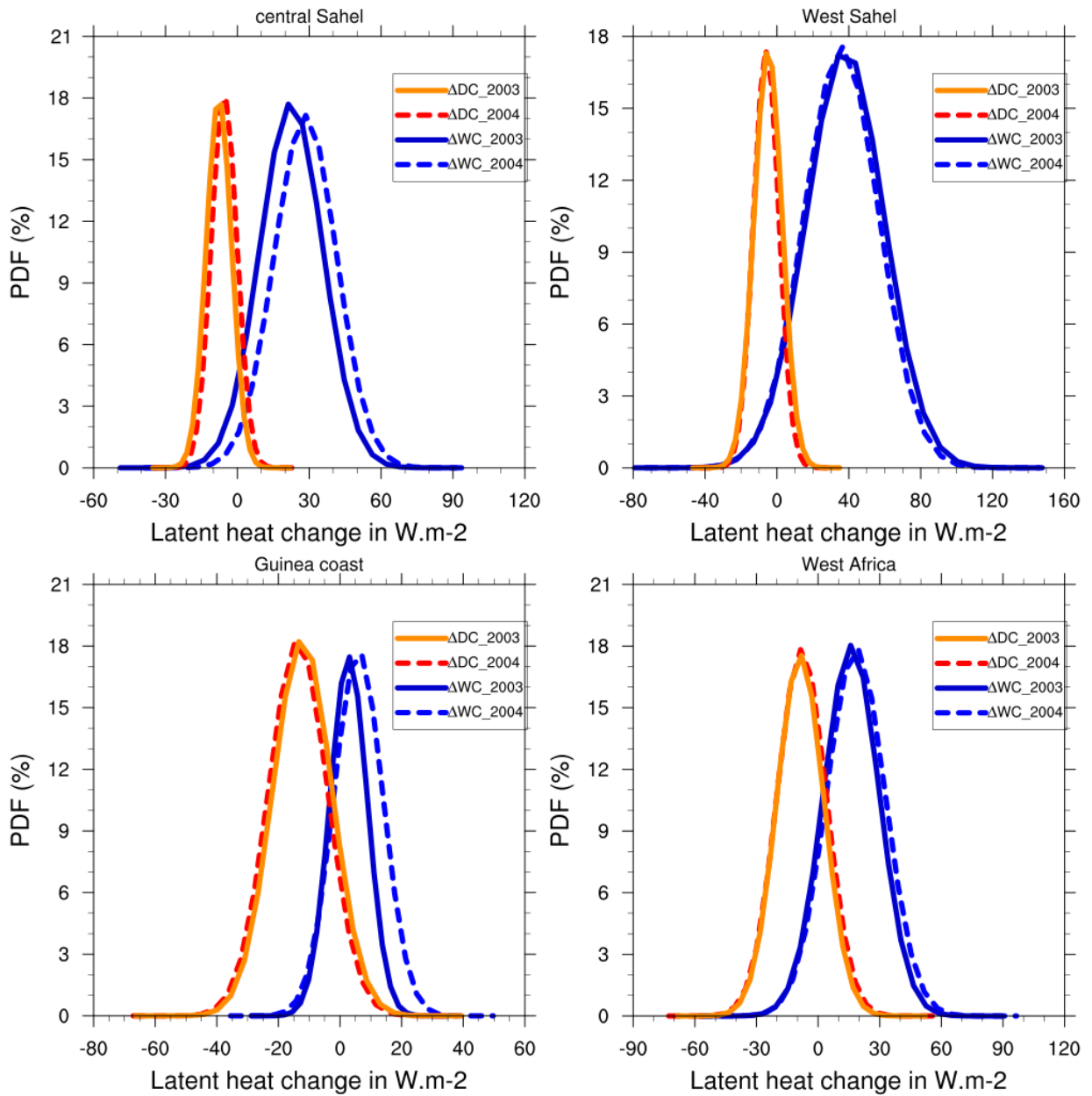
970
971
972
973
974



975
976
977
978
979
980
981
982
983
984
985
986
987

Figure 16: Same as Fig.12 but for latent heat fluxes (in $W \cdot m^{-2}$).

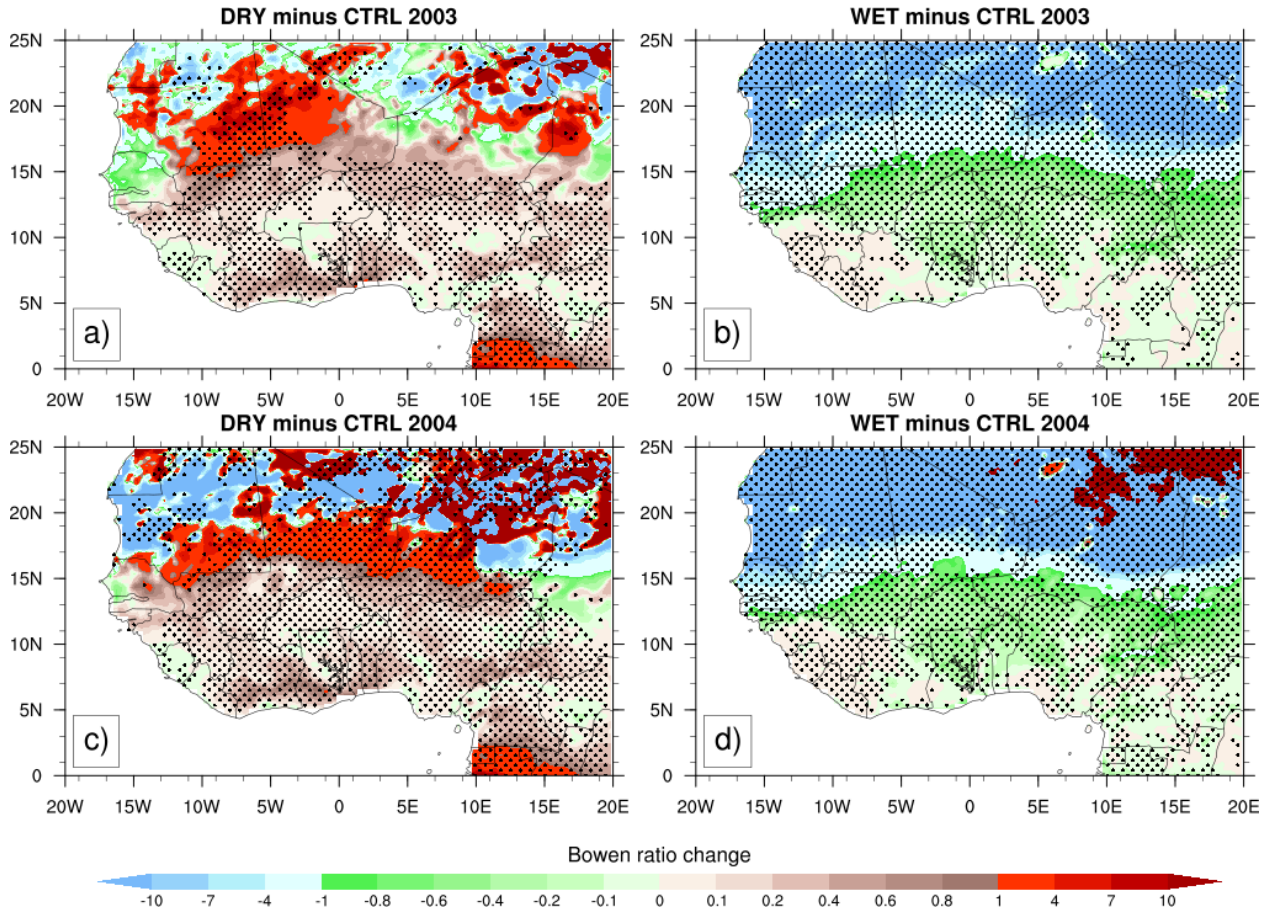
988
989
990
991
992



993
994
995
996
997
998
999

Figure 17: Same as Fig.13 but for latent heat fluxes (in $W.m^{-2}$).

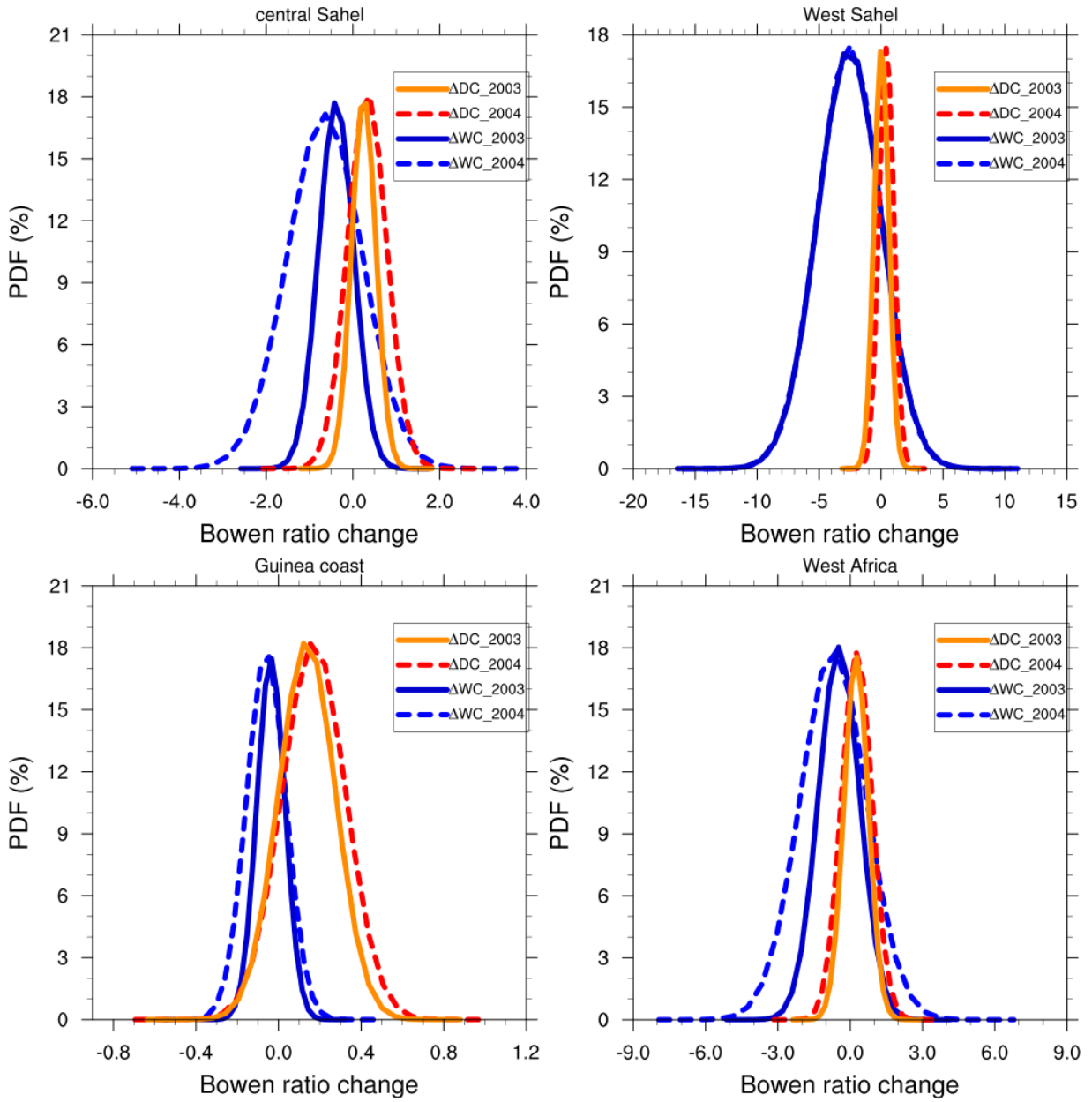
1000
1001
1002
1003



1004
1005
1006
1007
1008
1009
1010
1011
1012
1013
1014
1015
1016
1017

Figure 18: Same as Fig.12 but for Bowen ratio.

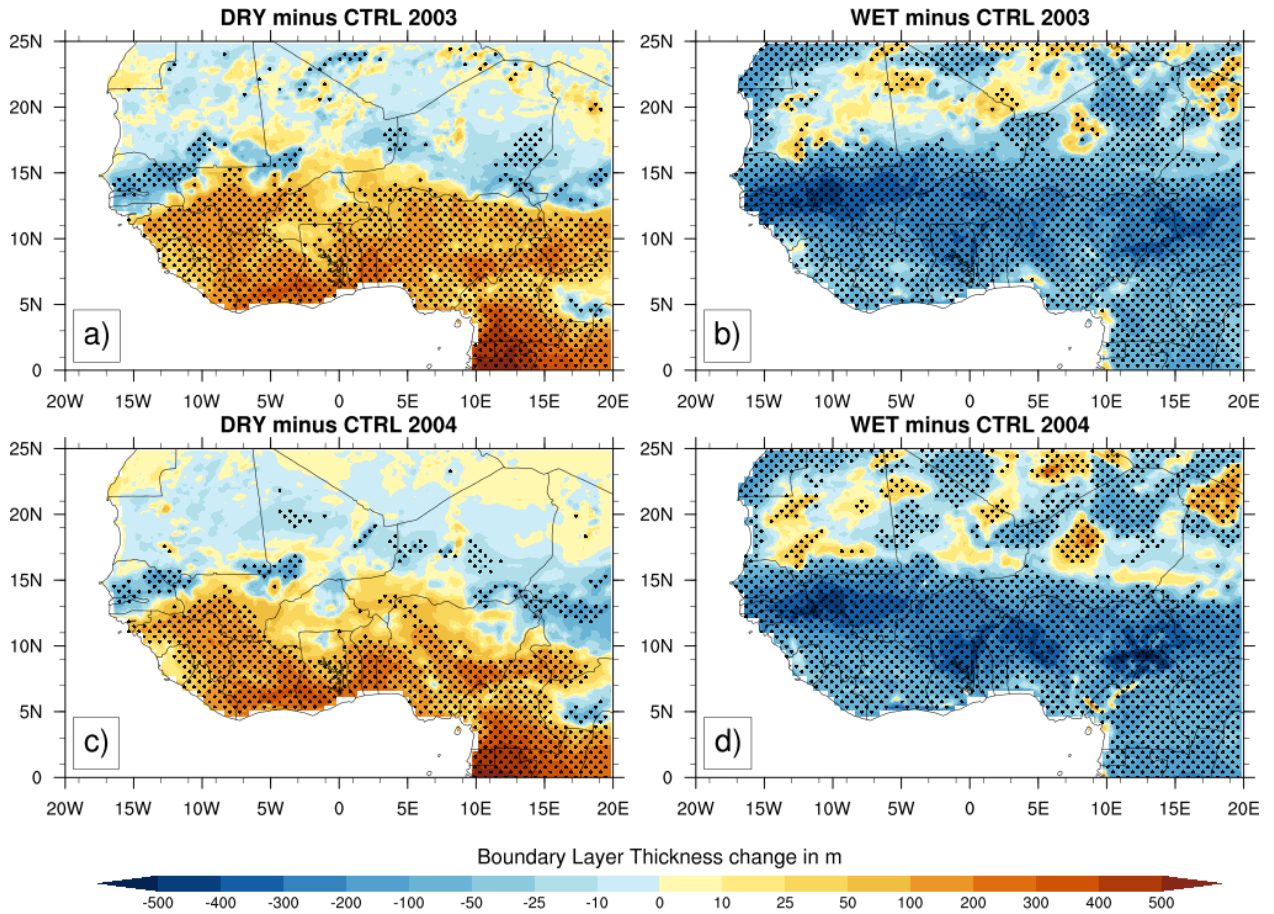
1018
1019
1020
1021
1022
1023



1024
1025
1026
1027
1028
1029

Figure 19: Same as Fig.13 but for Bowen ratio.

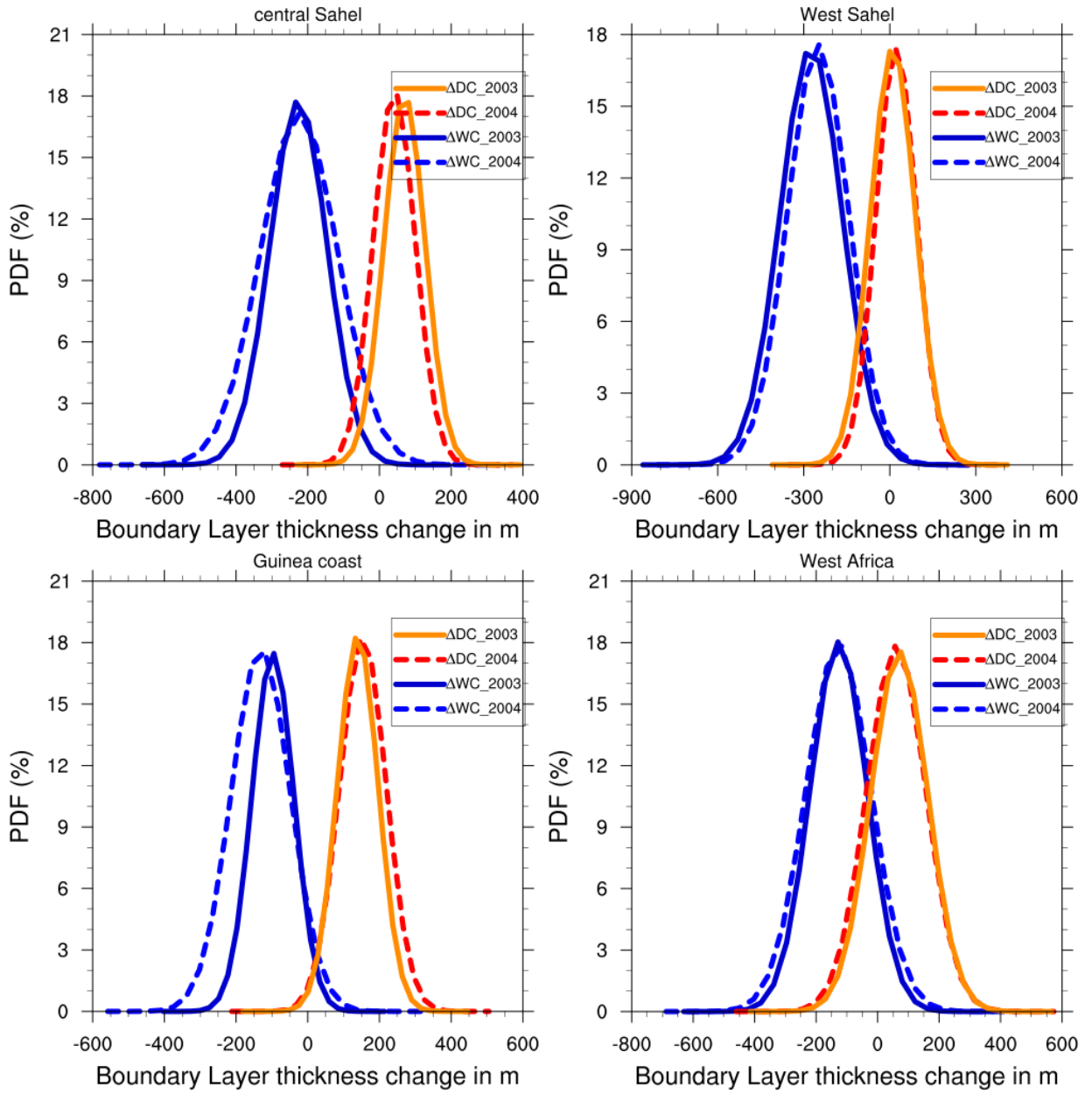
1030
1031
1032
1033
1034



1035
1036
1037
1038
1039
1040
1041
1042
1043
1044
1045
1046
1047

Figure 20: Same as Fig.12 but for the change of the height of the planetary boundary layer (in m).

1048
1049
1050
1051
1052



1053
1054
1055
1056
1057
1058
1059

Figure 21: Same as Fig.13 but for the height of the planetary boundary layer (in m).

1060

1061

1062